Effect of Protein Interactions on the UHMWPE Composites After the Multidirectional Wear Test

Nur Hidayah Shahemi
Universiti Teknologi Malaysia
SHAHIRA LIZA KAMIS (shahiraliza@utm.my)
Universiti Teknologi Malaysia https://orcid.org/0000-0002-5282-1893
YOSHINORI SAWAE
Kyushu University: Kyushu Daigaku
Takehiro Morita
Kyushu University: Kyushu Daigaku

Research Article

Keywords: UHMWPE, Hydrophobicity, Surface charge, Surface free energy, Thermal conductivity, Protein Adsorption

Posted Date: March 4th, 2021

DOI: https://doi.org/10.21203/rs.3.rs-266241/v1

Effect of protein interactions on the UHMWPE composites after the multidirectional wear test

N. Shahemi[1], S.Liza[1*], Y. Sawae[2], T. Morita[2]

[1]*TriPreM i-Kohza, Department of Mechanical Precision Engineering, Malaysia-Japan International Institute Technology, Universiti Teknologi Malaysia, 54100, Kuala Lumpur, Malaysia.*

[2]*Machine Elements and Design Engineering Laboratory, Department of Mechanical Engineering, Faculty of Engineering, Kyushu University, 819-0935, Fukuoka, Japan.*

**Corresponding author*: shahiraliza@utm.my

Abstract

Recent studies have found a rapid increase of ultrahigh molecular weight polyethylene (UHMWPE) wear in the presence of proteins from the synovial fluid. This is due to the high hydrophobicity surface of UHMWPE which allows the proteins to get interacted and adsorbed to the UHMWPE surface. Moreover, since UHMWPE has low thermal conductivity, the heat elevated produced from the articulating contact surfaces would be slowly dissipated and protein structure becoming denatured. The denatured proteins were claimed could increase the adhesive wear response. Thus, the main objective of this study is to evaluate the influence of the graphene oxide (GO) and graphite flake (GF) on the UHMWPE's heat dissipation and wettability characteristics in regards to reducing the protein denaturation effect on the surface. The surface properties were characterized by using surface energy evaluation, zeta potential, and Fourier Transform Infra-red (FTIR). Following that, wear properties of each UHMWPE composite were evaluated by using a multidirectional pin-on-disc wear test under a lubricated condition. The worn surface of each pin sample was evaluated, and the dominating factors of wear properties were determined. In addition to that, the effect of protein absorption on the UHMWPE composites was also evaluated in this study. The results show both fillers (GO and GF) had no effect in altering the UHMWPE composites' physicochemical properties. The improvement of UHMWPE composite's wear properties was discovered to be primarily dominated by the existence of GO filler (1.0 wt%) near the sliding surface has improved the subsurface strength of the material and heat dissipation effect which reduces the denaturation of the proteins.

Keywords

UHMWPE; Hydrophobicity; Surface charge; Surface free energy; Thermal conductivity; Protein Adsorption.

1.0 Introduction

The wear debris formation from ultrahigh molecular weight polyethylene (UHMWPE) during articulating activities in joint replacement is highly influenced in reducing its lifespan to 15-20 years [1-2]. The adverse reaction of the wear debris to the surrounding tissues has led to bone degeneration (osteolysis), thus resulted in implant loosening. Several researchers have attempted in maintaining the excellent attributed properties of the polyethylene while increasing its wear resistivity by introducing filler reinforcement into UHMWPE or simply known as modification UHMWPE into a composite material [2]. Different types of fillers can be incorporated into the polymers depending on their material's properties and compatibility in functioning on the properties enhancement or at a particular application [2-4].

Other than striving for mechanical improvement to improve the wear properties, the UHMWPE composites were also prepared to resist wear while get interacted with the synovial fluid constituents. Since wear could also be initiated from several other factors such as the interaction of UHMWPE with the synovial fluid's constituents and elevated thermal during sliding activities at the surface contacting load. Recent studies have found a rapid increase of UHMWPE wear and friction response in the presence of proteins from the synovial fluid [5-6]. This is due to the high hydrophobicity surface of UHMWPE which allows the proteins to get interacted and adsorbed to the polyethylene surface [7]. Moreover, since UHMWPE has low thermal conductivity, the heat elevated produced from the articulating contact surfaces would be slowly dissipated [8]. Due to the soft protein structure, the elevated contact heat would unfold the structure of the protein, becoming denatured. The denatured proteins were claimed could change the polyethylene surface characters and forming high shear stress during the sliding activities. Hence, increasing the adhesive wear response.

Graphitic materials have unique sets of bonding that would be able to form with different kinds of biomolecules. But one of the winning point of this filler type is its hydrophilicity behaviour. Perhaps, with the type of chemical bonding existed in the graphitic materials, and the synergistic effect after the reinforcement, it may reduce the hydrophobicity of the composite [9-10]. Hence, may reduce the protein adsorption onto its surface. Furthermore, the reinforcement of high thermal conductivity of graphitic materials can improve the heat thermal conductivity of the composite [11]. Although, there are many previous studies have reported on the increasing thermal conductivity after the reinforcement of the graphitic filler materials, the relation between thermal conductivity and wear mechanism is rarely

discussed [8,12-13]. A higher thermal conductivity could dissipate surface heat due to the sliding much faster, and may reduce the effect of proteins denaturation.

Research studies in UHMWPE composites were studied since the 1970s, it is still yet to be commercialized as a bearing implant component, due to lack of studies covered the material's structural stability while being exposed in the physiological environment. Therefore, the main objective of this study is to characterize the influence of the graphene oxide (GO) and graphite fillers (GF) on the UHMWPE's heat dissipation and wettability characteristics in regards to reduce the protein denaturation effect on the surface. Therefore, in this study data collection and analysis would be derived from the simulated hip kinematics and lubrication condition. The analysis was highlighted on the wear resistivity and the solid surface interaction with proteins. This research scope has driven the author to explore the feasibility of GF and GO reinforced UHMWPE composites for enhanced wear properties as a new type of joint prosthesis bearing material.

2.0 Materials and methods

2.1 Synthesis of UHMWPE based composites

Medical grade UHMWPE GUR 4120 used in fine powder form, with average particle size of 120 µm, average molecular weight 4.7×10^6 g/mol and density of 0.93 g/cm^3. It is supplied from the medical grade UHMWPE supplier from Fortron Industries, LLC, Germany. The graphitic-based fillers used in this study are graphite flakes (GF) and graphene oxide (GO) respectively. GF purity is 99.60% with average particle size 48 µm, and average molecular weight is 1.201×10^{-3} g/mol (ACS Material, LLC, California, USA). GO used with purity > 95 wt%, average particle size of 10 - 30 µm and average molecular weight 4.239×10^{-5} g/mol (Xiamen Tob New Energy Technology Co. Ltd). By varying the proportion of each filler; GF and GO with the amount of 0.1 wt% and 1.0 wt% were added into the UHMWPE matrix to avert a severe particle agglomeration in the composite structure [14].

The composite samples were prepared using conventional method which involved powder melt-blending and hot pressing. First and foremost, ratio of matrix powder and filler were calculated according to the weight percentage of filler (0.1 and 1.0 wt% respectively) as tabulated in **Table 1** and hot press mold volume; 1.35 cm^3. Then, the matrix powder and filler

were blended using dry blender to ensure an even mixing for 15 minutes. Initially, temperature of polymer composite processing is refined according to UHMWPE's melt process ability temperature; 185 °C. By using double rotation mixer from Duplex Sigma Kneader, Russia, the mixed powder (UHMWPE and filler) were melt blended at 185 °C for 60 minutes.

Table 1 List of composite samples prepared

Sample name	Graphitic-based fillers	
	GO (wt%)	GF (wt%)
UHMWPE	0	0
UHMWPE/0.1GO	0.1	0
UHMWPE/1.0GO	1.0	0
UHMWPE/0.1GF	0	0.1
UHMWPE/1.0GF	0	1.0

Following to the melt-blending process, the blended mixtures were compressed with hot-pressing machine at 180 °C, 10 MPa for 45 minutes into 150 × 150 × 6 mm sheet. The fabricated sheets then machined into pin with dimension of 5 × 5 × 15 mm for multidirectional pin-on-disk wear test. Finally, the hot-pressed sample were cold-pressed at room temperature, 10 MPa for 15 minutes. Cold press method is to allow recrystallization of polymer composite after heated.

2.2 Characterization of modification effect on surface properties

The surface properties of the modified UHMWPE were investigated due to the hydrophilicity of the GO and GF. It is well known that protein has become a major effect of UHMWPE wear degradation in the physiological environment due to its high hydrophobicity behaviour [7]. Its hydrophobicity attracts a different kind of protein structure to be adsorbed and due to its soft structure, it will denature and altered the surface properties, which will form high stress and increase the adhesive wear response. Hence for this part of the study, the synergistic effect of the filler on altering the surface properties of the UHMWPE polymer was evaluated and analysed accordingly.

2.2.1 Wettability of modified UHMWPE

Single drop (3µL) of 30 v/v% diluted fetal bovine serum (FBS) is dropped onto the surface of UHMWPE, UHMWPE/GF and UHMWPE/GO with a dimension of 100 × 25 × 2 mm were used to measure the contact angle of the bovine serum with the sample surfaces. Five

(5) readings of contact angle were taken on each sample using an optical system of high-resolution camera known as charge-coupled device camera (CCD). The contact angle was measured using the Laplace-Young method by using Equation (1), where *h* is the height and *D* is the diameter of the droplet [15]

$$\theta = 2\ arc\ tan\frac{2h}{D} \tag{1}$$

2.2.2 *Surface free energy of modified UHMWPE*

The contact angle of the samples was measured using three different liquids with known polar (γ^p), dispersive (γ^d) and hydrogen (γ^h) components of the solid surface. The hydrophobicity behavior and the type of interactions happening with a different type of surface component will be determined in a quantitative manner by using extended Fowkes method was used as shown in Equation (2) [16].

$$\begin{pmatrix} \sqrt{\gamma_s^d} \\ \sqrt{\gamma_s^p} \\ \sqrt{\gamma_s^h} \end{pmatrix} = \begin{pmatrix} \sqrt{\gamma_l^d}, A & \sqrt{\gamma_l^p}, A & \sqrt{\gamma_l^h}, A \\ \sqrt{\gamma_l^d}, B & \sqrt{\gamma_l^p}, B & \sqrt{\gamma_l^h}, B \\ \sqrt{\gamma_l^d}, C & \sqrt{\gamma_l^p}, C & \sqrt{\gamma_l^h}, C \end{pmatrix} \begin{pmatrix} \gamma_l, A\ \frac{(1+\cos\theta_A)}{2} \\ \gamma_l, B\ \frac{(1+\cos\theta_B)}{2} \\ \gamma_l, C\ \frac{(1+\cos\theta_C)}{2} \end{pmatrix} \tag{2}$$

where γ_s and γ_l are the surface energy of solid and liquid respectively, γ^d ,γ^p, γ^h referring to dispersion, polar and hydrogen forces respectively. Meanwhile, A, B, and C representing the three different liquid used for component quantifications in the experiment; which are distilled water, hexadecane, and diiodomethane respectively. The surface free energy of the liquids used into the extended Fowke's calculation was tabulated in **Table 2.**

Table 2. Surface free energy of the liquids used in extended Fowke's calculation [16-17].

Test liquid	Surface energy (mN m^{-1})			
	γ^d	γ^p	γ^h	γ^T
Distilled water	29.1	1.3	42.4	72.8
Hexadecane	27.9	0	0	27.9
Diiodomethane	46.8	4.0	0	50.8

2.2.3 Surface charge measurement

Protein adsorbs onto solid surfaces not only through the hydrophobic surface but electrostatic interactions as well. Electrostatic interactions are depending on solid surface charge and protein charge. Proteins charge is generally controlled by pH value, where high pH value will make the proteins to be negatively charged and low pH value will make the proteins to be positively charged. Bovine serum albumin (BSA) as the protein source (Gibco, Life Technologies Limited, UK, Cat. No. 11020-021) was used. In this study, the pH value of BSA is maintained in a range of 7- 7.6 which is the same as pH value in human synovial fluid. Hence, in determining the protein albumin charge in higher confidence, the measurement of proteins' potential difference was performed using the zeta (ζ) potential test. The composite samples' potential difference was also determined using the same method. ζ potential is the measurement of the materials' electrophoretic mobility in tetrahydrofuran solvent which calculated using the Henry **Equation (3)**:

$$\nu = \frac{2\varepsilon\zeta}{3\pi\eta}\,[f(\kappa\alpha)] \qquad (3)$$

where ν is the electrophoretic mobility, ε and η are the dielectric constant and the viscosity coefficient of the solution surrounding the colloid particles, respectively and f (κα) is the correction factor.

2.2.4 Protein adsorption test at static condition

Static protein adsorption analysis was simulated by allowing the sample to be immersed in the protein solution and interacted according to the standard protein adsorption protocol from Sigma Aldrich. BSA as the protein source was used same as in the section 2.2.3. UHMWPE and UHMWPE composites were prepared with a dimension of 5 × 10 × 2 mm. Each sample is soaked with 2 wt% BSA solution in a sterilized petri dish. The petri dish was then incubated at 37 °C, 5% of CO_2 controlled atmosphere, 95% humidity for 24 hours. Protein seeded samples were then washed with distilled water to remove non-adherent protein. Then, the samples were washed with phosphate-buffered saline (PBS) solution (Gibco, Life Technologies Limited, UK, Cat. No 10010-023) to maintain the physiological pH (7-7.6). Optical microscope was used to observe the proteins adsorbed on the surface, Attenuated Total Reflection-Fourier

Transform Infrared (ATR-FTIR) microscope (ThermoScientific Nicolet iN10 MX FT-IR) equipped with germanium ATR objective was used to verify the denaturation of the protein on the solid surface and energy dispersion spectroscopy (EDS) was used to note the protein element percent existed in a 100 µm × 100 µm surface area of each sample. Proteins' coverage area percentage was measured using ImageJ software.

2.3 Thermal conductivity measurement

Thermal conductivity measurement can be calculated using differential scanning calorimetry (DSC, Mettler Toledo, Germany) under a nitrogen atmosphere with a flow rate of 10 mL/min. The temperature and heat flow signals from calorimeter were calibrated using indium and zinc standards prior to testing. Each sample was weighed between 5 mg to 7 mg in a disc-shaped aluminum pan and heated from 30 to 200 °C at a heating rate of 10 °C/min. The thermal conductivity of the material is quantified by the thermal conductivity parameter by defining the time taken of material to diffuse heat. The energy fraction passing through the material is known as heat flux. The combination of other parameters such as surface, the position of heat diffused, and time taken was concluded in the Equation (4) as referred from previous studies [11,18].

$$\kappa = \alpha . C_p . \rho \qquad (4)$$

where κ is the thermal conductivity (W. m^{-1} K^{-1}), α thermal diffusivity ($m^2.s^{-1}$), C_p is a specific heat capacity ($J.K^{-1}kg^{-1}$) and ρ is the density of the material.

2.4 Multidirectional wear sliding test

The wear behavior of UHMWPE composites sliding against a medical-grade CoCrMo metal disc was evaluated by using a three-station multidirectional sliding pin-on-disk wear tester. The wear test was developed in Kyushu University [6] to simulate the hip joint application sliding motion which has the same basic principle as the Saikko's CTPOD device [19]. The composite pin samples were attached individually in each station into a loading bar. Each station has a separate liquid bath which was moved by a motor and crank mechanism caused the attached pin sample articulates upon the CoCrMo disc in a circular motion path with a 30 mm diameter. The contact stress used in this study was 5 MPa; which equivalent to contact load, 125 N. The contact stress was selected at the particular value to simulate the least and the

average value of von Mises stress under dynamic walking conditions acted upon the UHMWPE composites [20]. For the lubrication of the wear test, 30 v/v% of FBS was used. The diluted FBS used in this study contained a protein concentration of 1.1 wt%; which has about the same range of macromolecules concentration as the synovial fluid in the human body [21-22]. The sliding test was performed according to the parameters in **Table 3**.

Table 3 Experimental conditions for wear test using 5 MPa contact load.

Parameters	Value
Contact pressure (MPa)	5.0
Contact load (N)	125
Speed (mm/s)	50
Sliding distance (km)	10
Operating temperature (°C)	25
Lubricant type	Diluted 30 v/v FBS

2.3.1 Specific wear rate

The specific wear rate was calculated from the volume loss of the pin specimens divided with the sliding distance. The wear volume was firstly measured at the first 5 km sliding interval using weight balance with an accuracy of 0.001 mg divided by the respective samples' density measured by the density meter (Shimadzu SMK-401, Japan). By using the same respective pin sample, the wear test was then continued to finish the remaining 5 km sliding and completed a total 10 km sliding distance. In order to give a significant outcome especially in a clinical wear perspective, in this study, the observation on the wear rate for the first 5 km interval sliding distance has become as important as the total wear debris production. This is because a high wear rate obtained only after sliding for a short distance could frequently be correlated with creep deformation, which has a high potential in increasing the risk of implant's early failure upon implantation [23-24].

2.3.2 Protein adsorption analysis post wear test

All samples that underwent the sliding test was further tested to compare the protein influence on the wear properties. The worn surface of each sample was analysed using ATR-FTIR. Amide I and Amide II spectrum peak would be scanned, and the infrared wavelength

was focused within range of 1800 cm^{-1} to 1500 cm^{-1}. The difference between peaks were analysed and discussed.

3.0 Results and discussion

3.1 Surface properties of modified UHMWPE

Surface properties characterization is needed to understand the initial protein's interaction with the UHMWPE composite samples. The following investigations were performed to understand the effect of each filler in reducing the interaction with the proteins before the contact loading and frictional heat effect during the sliding test. The discussions were involved concerning the changes in their surface chemistry and surface charge.

3.1.1 Wettability

The surface wettability was determined by measuring the contact angle of diluted FBS on each sample's surface. A contact angle with less than 90° is considered to be relatively high wettability, while a higher contact angle than 90° would have lower wettability. 30 v/v% FBS was used for the wettability test instead of water as it has close similarities to synovial fluid in regards of their constituents' percentage and has been widely used to simulate the biological environment of the joint application [25-26]. Other than that, a good wettability between implant materials and FBS indicate a higher chance of macromolecules attraction that work in the host defense mechanism such as macrophages [27] and other foreign microorganisms, which limiting active binding site for protein adsorption on the implant's surface. Hence, the interaction's improvement between the sample and FBS is crucial.

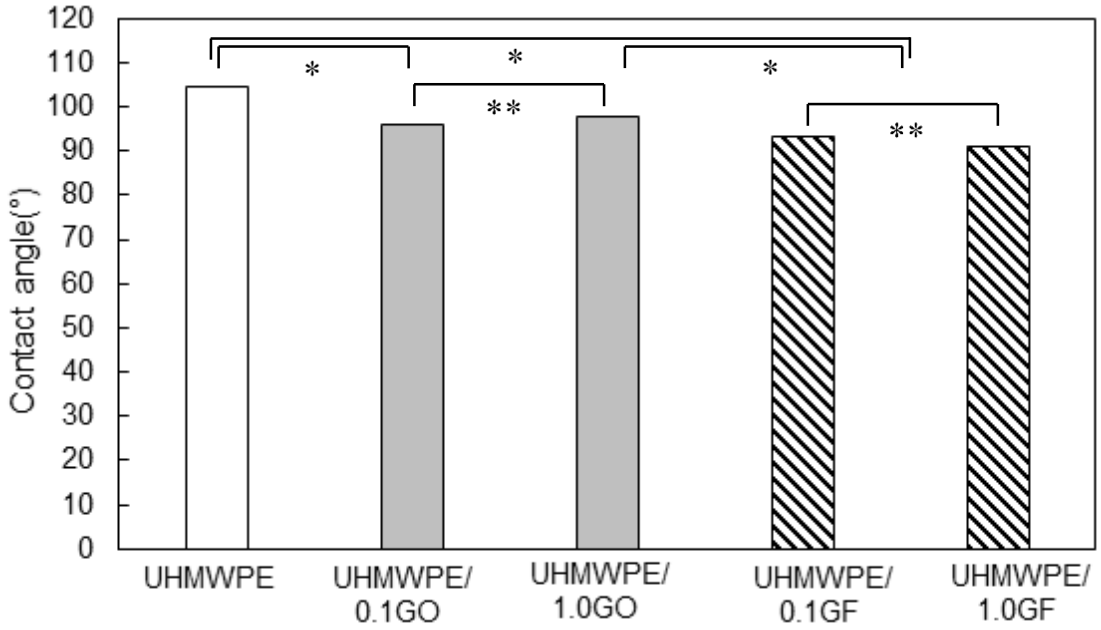

Fig. 1. The contact angle of UHMWPE, UHMWPE/GO and UHMWPE/GF composites at different filler contents; where (*) denotes no significant difference ($p>0.05$) and (**) denotes significant difference ($p<0.05$)

From **Fig. 1** we can observe that the contact angle of UHMWPE is the highest compared before being modified into composites; 104 ± 1°. After reinforcing GO into the UHMWPE at 0.1 wt% and 1.0 wt%, the contact angle was significantly reduced ($p>0.05$) to 97 ± 1° and 96 ± 1°, respectively. Meanwhile, the incorporation of GF at the same concentration has led to further reduction of contact angle which is 93 ± 1° and 91 ± 1°, respectively. Although the reinforcement of these fillers has proven to increase the surface wettability, higher amount of the filler doesn't have any significant differences ($p >0.05$) for further wettability improvement. Respective to the contact angle measurement, the composite materials have shown an increasing wettability behaviour and UHMWPE/GF composite sample exhibit the highest wettability amongst the other sample. Followed by UHMWPE/GO and UHMWPE showed the lowest wettability. The wettability of the sample was likely to be elevated by surface chemical composition on the surface or/and the physical interaction between the FBS and solid surface morphology [28-29]. However, the interactions of the bovine serum with the surface can't be specifically determined by comparing the magnitude of the contact angle alone. Therefore, the surface free energy of the composite samples was evaluated to investigate the existence of different interactions on the samples' surface. Hence, the dominating factors affecting the wettability of the composites' samples can be confirmed.

3.1.2 Surface free energy

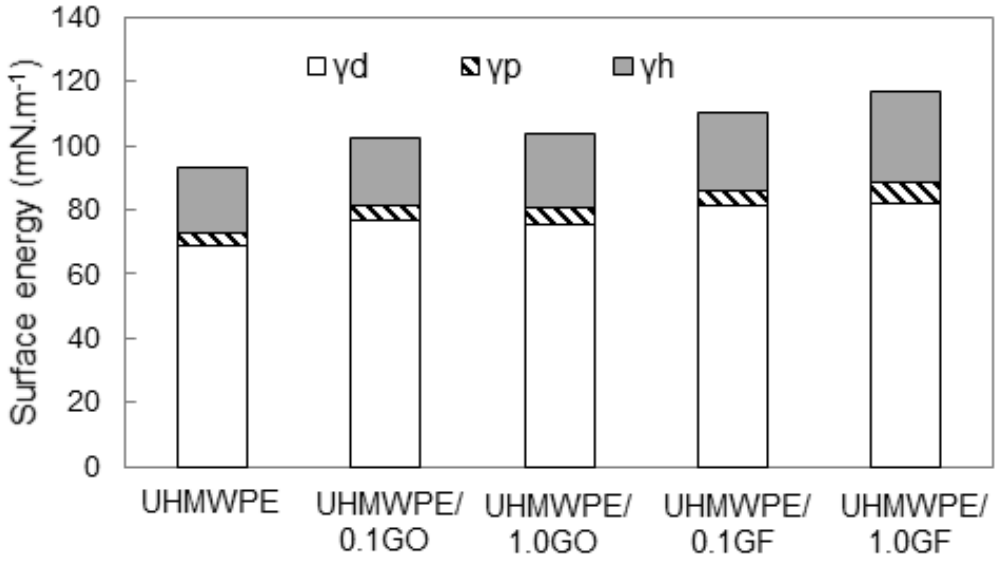

Fig. 2. Surface free energy of UHMWPE and UHMWPE/GO and UHMWPE/GF composites at a different filler content

Fig. 2 shows surface free energy of UHMWPE and UHMWPE/GO and UHMWPE/GF composites at a different filler content displayed the changes in surface free energy with the incorporation of GO and GF fillers in the UHMWPE. The surface energy of UHMWPE has increased from 93.1 mN/m to 102.6 and 103.8 mN/m when added with 0.1 wt% and 1.0 wt% GO particles respectively. Meanwhile, when UHMWPE was added with GF at the same increasing wt%, the surface energy has increased to 110 mN/m and 116.5 mN/m respectively. UHMWPE/1.0GF shows the highest surface energy among all composite samples. These findings indicate that UHMWPE/1.0GF has the least hydrophobic properties followed by UHMWPE/0.1GF, UHMWPE/1.0GO, UHMWPE/0.1GO, and UHMWPE display the most hydrophobic behavior. The reduction of the samples' hydrophobicity was further analyzed by the type of surface interactions; polar (γ^p), hydrogen (γ^h), dispersive (γ^d) component. However, based on **Fig. 2**, there was no apparent increment of γ^p or γ^h between the UHMWPE and the composite samples that can be noted. On the contrary, the slight increment of γ^d was measured when the fillers were added. This indicated that the physical interaction between the testing fluids is mainly contributed to the hydrophobicity reduction of the UHMWPE composites as opposed to their surface chemistry. The physical interaction between the testing fluids and the surface morphology of the samples was likely to be encouraged due to the existence of temporary electrons on the sample surface [28-29], which allow the fluids to have a relatively

higher affinity of spreading. Hence, the reduction of hydrophobicity of the UHMWPE composites can be concluded to be highly influenced by the increasing physical interaction with the surface area albeit the resultant of polar interactions with the sample surface was initially expected.

3.1.3 Surface charge

Proteins adsorption onto the samples are not solely dependent on the hydrophobic behavior alone [6,10,30]. Proteins adsorption is also influenced by the electrostatic interactions between the sample surface and the protein charges. The attraction force is produced when two interfaces are oppositely charged, resulted in easier protein interaction and adhesion, whereas the same charges will cause repulsion force and make the protein adhesion to be less likely favoured [31]. However, other than the existence of proteins recognized in the FBS, it has also consisted of different other constituents such as hyaluronic acid and also several kinds of lipids [25]. Thus, in order to effectively studying the specific electrostatic interaction between proteins structure and the composite samples, BSA was used in this study.

BSA protein was chosen as it is make up the 60% of proteins percentage amongst all other different types of proteins such as immunoglobulin, fibrinogen, and lysozyme [27,32-33], and was found to have contributed the highest interaction with implanted materials [32]. Protein charge is usually found to be influenced by a function of pH [34-35]. Low pH proteins are positively charged and high pH proteins are negatively charged [35]. However, in this study, the pH value of BSA proteins used will be fixed as the same range as the human synovial fluid; pH 7-7.6 [21]. Since the isoelectric points (net charge) of protein is usually found around pH 4 [34], hence, it is expected for BSA to have a negatively charged molecules. Nonetheless, zeta potential measurement was used to determine the BSA's charge for higher confidence. Zeta potential evaluation was also performed on all dissolved samples as can be seen in **Fig. 3**.

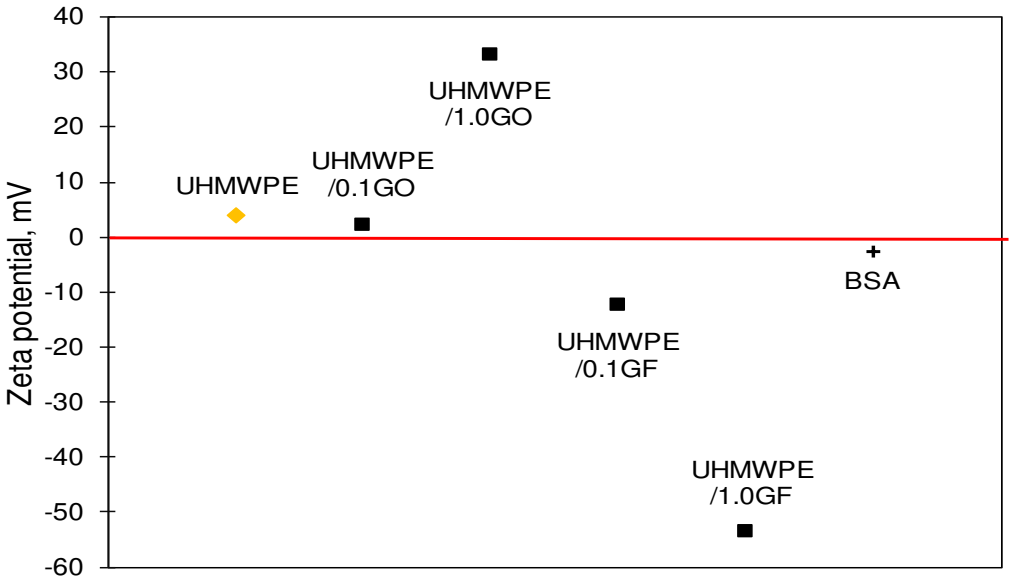

Fig. 3. Surface charge of UHMWPE and UHMWPE/GO and UHMWPE/GF composites at different filler content.

UHMWPE, UHMWPE/0.1GO and UHMWPE/1.0GO have shown positive zeta potential value of +4.08 mV, +2.17 mV and +32.93 mV respectively, meanwhile, UHMWPE/0.1GF, UHMWPE/1.0GF and BSA exhibit negative ζ potential value of -12.57 mV, -53.61 mV, - 2.71 mV. UHMWPE filled with GF exhibited a negative ζ potential value due to the incorporation of the negatively charged surfactant particles which believed to be adsorbed on GF during the exfoliation process [36-37]. By looking from the electrostatic interaction standpoint, from this finding, it indicated that BSA is most likely to be adsorbed onto the UHMWPE and UHMWPE filled with GO filler due to their oppositely charged, meanwhile the same charge of BSA with UHMWPE/GF samples produced repulsive force. This result is expected due to the facts that all proteins membranes have high amount of negative charges compared to positive charge [21,34], however, proteins can also interact on near-neutral and negative surfaces but happens only at certain conformation type [27]. The high positive or high negative ζ potentials greater than 30mV lead to monodispersity, meanwhile, small magnitude, <5mV can lead to poor dispersibility [38]. The poor dispersibility attributed to the formation of randomly ordered mixed monolayer of both interfaces, which effectively cancels out the electrostatic potential induced by either interface [38]. This means, when two interfaces have the opposite charge with low magnitude, they will likely cancel out each other's electrostatic potential causes agglomerations [39]. For example in this study, the proteins' agglomeration is prospectively induced from the interaction between UHMWPE and BSA protein, and UHMWPE/0.1GO with BSA proteins because of their oppositely charged, with

low magnitude. Therefore, based on the finding, it is expected BSA protein would likely to get interacted with the UHMWPE and UHMWPE/GO due to their opposite surface charge. The adsorption of proteins on the surface was further proven by performing the protein adsorption test at static condition.

3.1.4 Protein adsorption effect at static condition

Protein coverage area

Due to the aptness of proteins structure to change dependently on the environmental or stress condition such as pH environment, contact load, sliding speed and temperature [34,37, 40-41]. An in-vitro static condition for the protein adsorption was set up in order to understand its dominating factor when there are no external stresses. The interaction between the proteins and the sample surface would solely depend on the UHMWPE composite's surface chemistry. The proteins adsorbed on the surface would be visible to naked eyes due to its opaque appearance of macroscopic phenotypes [39]. Therefore, the surface samples were observed under an optical microscope as can be seen in **Fig. 4**. Small black dots with different coverage areas on each sample's surface can be noticed.

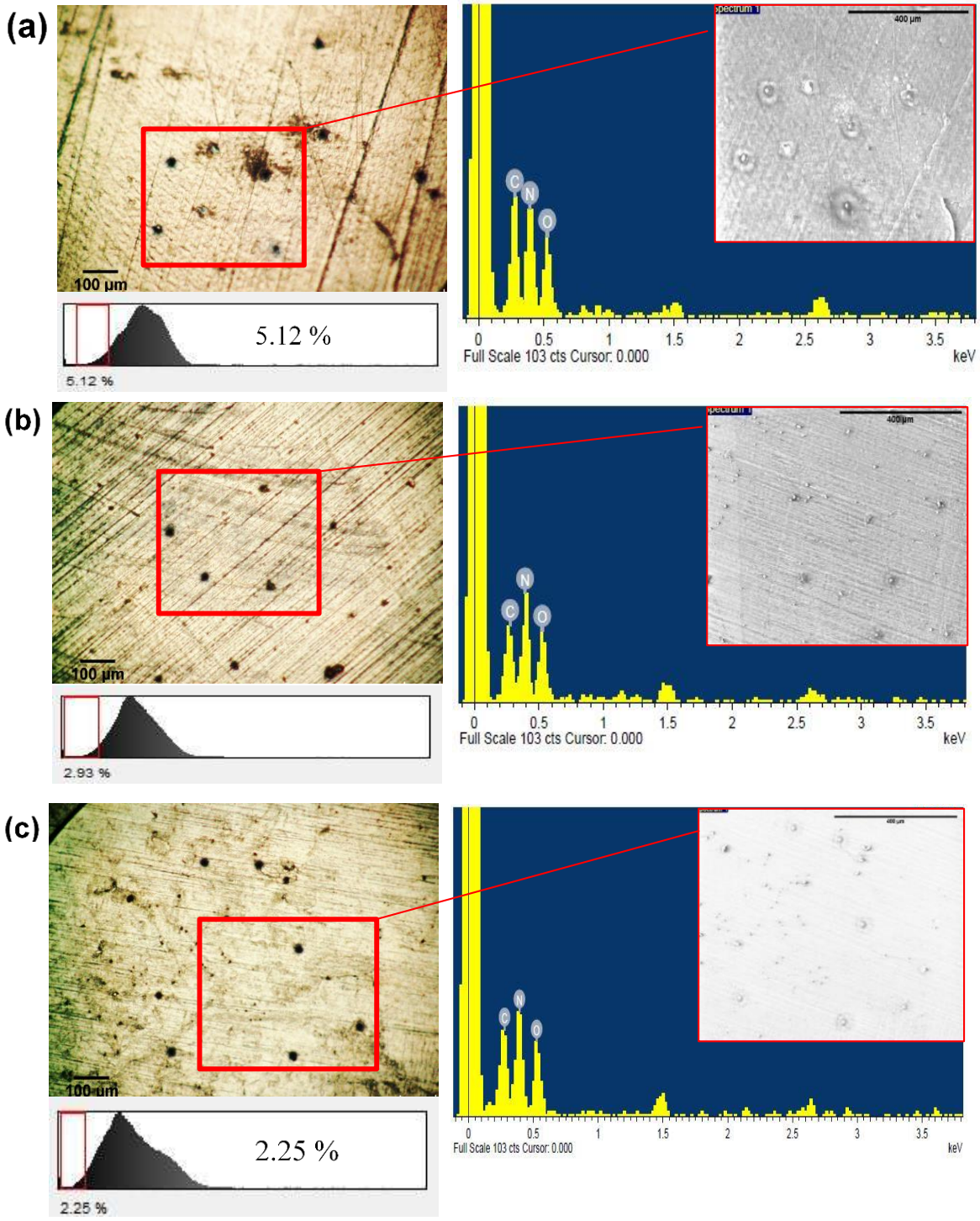

Fig. 4. Optical micrographs showed protein coverage on each sample surface (a) UHMWPE, (b) UHMWPE/0.1GO, (c) UHMWPE/1.0GO, (d) UHMWPE/0.1GF, (e) UHMWPE/1.0GF after 24 hr of incubation.

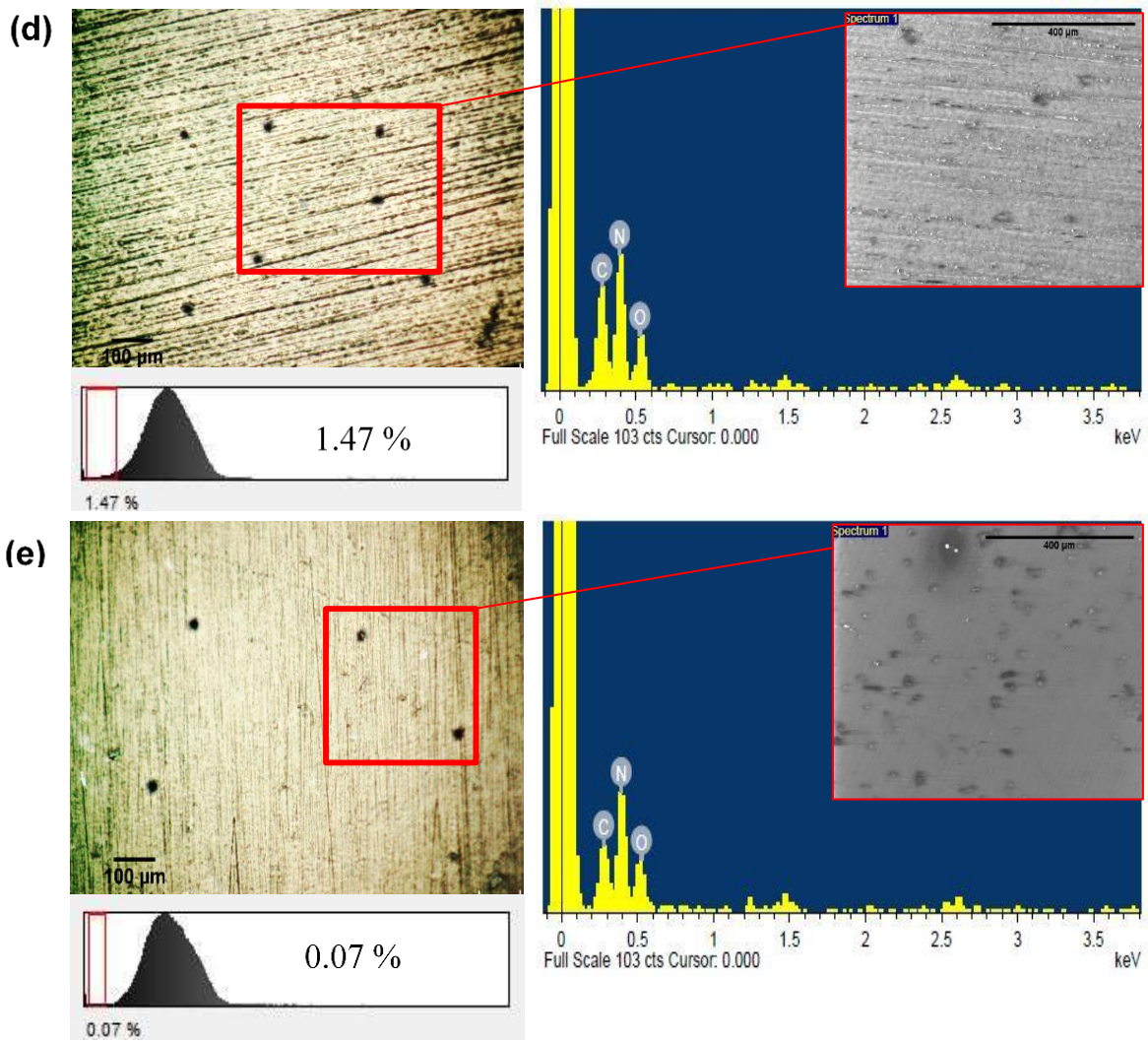

Fig. 4. (cont.) Optical micrographs showed protein coverage on each sample surface (a) UHMWPE, (b) UHMWPE/0.1GO, (c) UHMWPE/1.0GO, (d) UHMWPE/0.1GF, (e) UHMWPE/1.0GF after 24 hr of incubation.

The black dots were identified as nitrogen (N) using EDS in backscattered mode analysis. Nitrogen element is one of the major protein's elemental composition in the amide group [42], thus, the black dots can be assured as the major elemental constituents in the proteins. The data obtained from the microscope was analyzed by evaluating the protein's coverage from each sample's surface area using a threshold tool in ImageJ software. From **Fig. 4**(a), we can generally see that UHMWPE has the highest coverage area percentage (5.12%) and less disperse proteins albumin compared to the other composite samples. Moreover, UHMWPE/0.1GO and UHMWPE/1.0GO were observed to have a comparable protein coverage area percentage, which is 2.93% and 2.25% respectively and the proteins can be observed to be fairly disperse compared to the UHMWPE. Meanwhile, for UHMWPE/0.1GF, lower coverage area percentage (1.47%) of protein structure can be observed, whereas the

protein's location has become more disperse than the UHMWPE. The protein coverage area percentage of UHMWPE/1.0GF was the lowest (0.07%) yet the dispersion was comparable with UHMWPE/0.1GF. In addition to that, despite having the same charge of potential difference as the proteins, UHMWPE/GF was also attracted a little percentage of proteins on their surface which perhaps due to the protein's low internal stability [22]. A low internal stability protein or also known as soft-structured protein generally tends to adsorb on all surfaces irrespective of electrostatic interaction by an owing gain in conformational structure [22].

The proteins coverage on the samples' surface can be summarized as UHMWPE > UHMWPE/0.1GO > UHMWPE/1.0GO > UHMWPE/0.1GF > UHMWPE/1.0GF. From the summarized data, the descending order of the proteins coverage area obtained was respectively correspond to the samples' respective surface properties; ascending order of hydrophobicity, oppositely charge with the proteins, and descending order of surface roughness. However, since it is known that the high concentration of adsorbed proteins does not highly contribute to the wear degradation unless the proteins were in denatured conformation [5,32,43]. Therefore, the proof of the protein's coverage percentage area is not enough in determining that the adsorbed proteins at static conditions will induce higher wear on the sample material. An optical microscope is only capable of detecting a 2-dimensional surface structure, therefore, it cannot be used to recognize and differentiate the protein's conformation or folding. Nonetheless, a complimentary analysis to identify the type of protein folding is highly required in order to differentiate the changes of protein structure adsorbed on the UHMWPE composite samples.

Conformation changes of proteins at static condition

Generally, there are two types of protein conformation that are possibly taking place on the solid surface after it was adsorbed. The adsorbed protein structure can possibly form either a reversible or irreversible manner. The reversible manner of proteins structure can be easily removed from the sample surface as an only minor area of the protein's surface get attached with the solid surface, whereas, the irreversible manner of the protein's structure indicates the structure has extended and conformed to the solid surface which also known as proteins denaturation. Proteins denaturation or the loss of proteins' structural stability has become quite a concern especially due to its influence in escalating the surface wear of the polyethylene

implant component [5,32,43]. Henceforth, in order to identify the propensity of structural denaturation, the intensity of amide I IR spectra was examined.

ATR-FTIR is a preferable tool for examining the secondary structure changes of proteins to gain insight into the protein's conformation by analyzing the peak of amide I spectra [32]. According to the previous study [32], by the influence of sliding motion speed between the bearing components, it will induce the denatured proteins to get aggregated and promotes wear of the polyethylene surface. However, in this study, it is crucial for the sample to have a surface properties dependent analysis in a static condition without external stress, in order to indirectly determine whether the deterioration of polyethylene implant material is majorly related to the patients' active lifestyle or simply due to the physicochemical interactions between the proteins and the implant materials alone. Henceforth, the unfolding protein structure mechanism was expected to be understood via the FT-IR spectral range (1500 -1800 cm^{-1}) analysis following the static protein adsorption test was performed in **Fig. 5**.

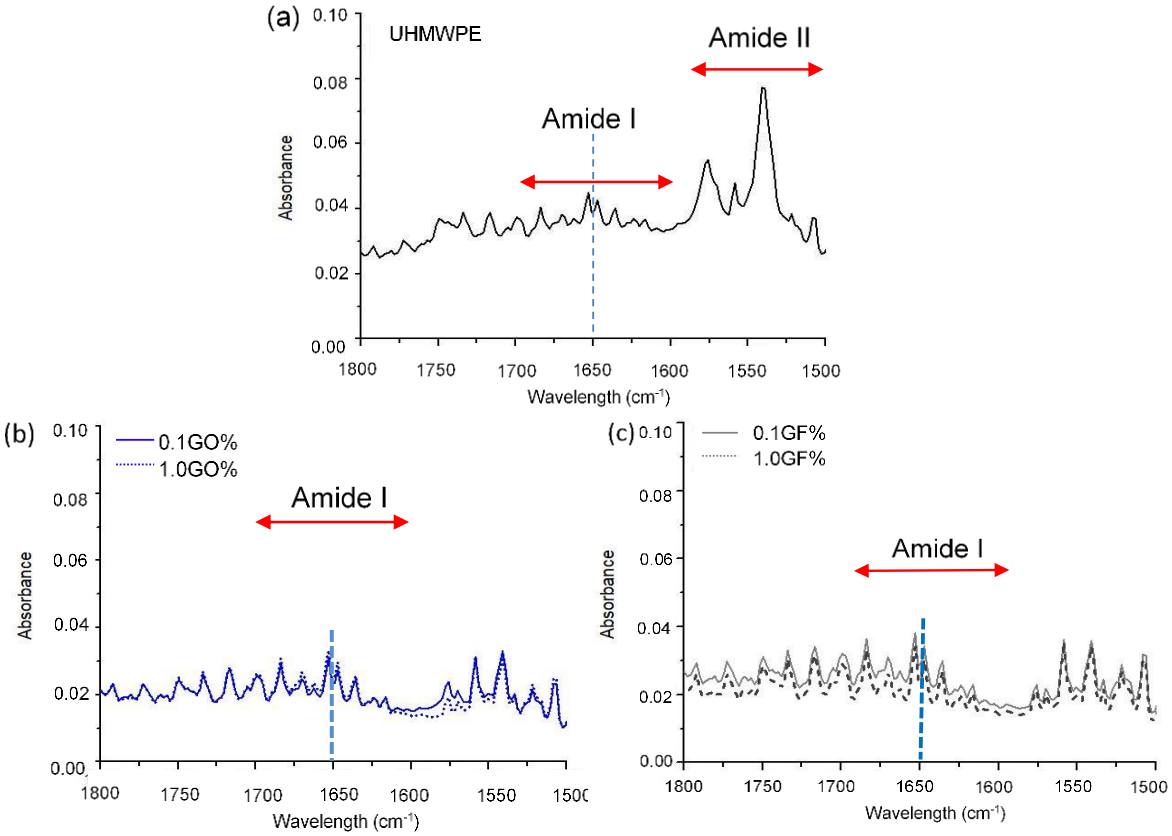

Fig. 5. ATR-FTIR spectra of proteins after 24 hr static condition in 2 wt% of BSA solution, (a) UHMWPE, (b) UHMWPE/0.1GO and UHMWPE/1.0GO, (c) UHMWPE/0.1GF and UHMWPE/1.0GF.

In **Fig. 5**, it showed that the intensity of IR spectrums was very weak and even a broad peak centered at 1650 cm^{-1} could easily be missed, but noticeable. The very small peaks and rough-textured IR spectrum are probably caused by a very small percentage of adsorbed proteins on the surface sample as previously displayed in **Fig. 4**. However, UHMWPE showed the most evident peak compared to the UHMWPE/GO and UHMWPE/GF in **Fig. 5**(b) and **Fig. 5**(c). Meanwhile, the peak of amide II in **Fig. 5**(a) can be significantly detected, unlike in sample **Fig. 5**(b) and **Fig. 5**(c) Though both amide I and amide II are sensitive to the secondary structure of proteins composition, the existence of amide II spectra is less useful to predict the number of secondary structures of proteins. This means that amide II as shown in the UHMWPE spectrum doesn't give any significant indication in the sample's data analysis, especially in a quantitative manner. However, given that the denaturation of the proteins was usually demonstrated by the decreasing intensity of the spectrum peaks in amide I region centered at 1650 cm^{-1}, which its characteristics obtained from unfolded proteins [32]. Therefore, the apparent peaks of the amide I and amide II spectrum observed on the UHMWPE surface validated the adsorption of proteins on the surface at static conditions. Thus, it suggested that UHMWPE has adsorbed higher protein compared to the other UHMWPE composite samples in a static condition. On the other hand, the lack of distinct peaks and its textured spectrums is suggested to be significant in determining the denaturing state of proteins structure detected on the UHMWPE composites' surface. As previously mentioned by Rabe et al., [27] in their review study, it was generally accepted that many proteins undergo conformational changes upon adsorption to a solid interface. Although proteins have favorable conformation state on the solid surface depending on the surface properties of the solid and only initially bind loosely on the solid surface, their surface affinity will increase afterward in time and changes its structure conformation [27].

This means, the conformational changes of the proteins on the UHMWPE composite surface are started since the adsorption event, and with the influence of time, desorption kinetics is further escalated. The same event was also applied on the UHMWPE/GF sample s even though it has the same surface charge as the proteins, which means that the hydrophobicity surface still the biggest influence when it comes to allowing the initial protein's interaction [38] on the UHMWPE composite surface. Hence, in this study, although the UHMWPE/GF samples have shown a slightly lower hydrophobicity compared to the other samples, it is not sufficient to deflect the protein's initial contact to the surface. Therefore, in a static condition, although the surface properties of the composites would definitely influence the adsorption of proteins

on the solid surface, the performance of 24 hours static protein adsorption test has allowed the conformation of the proteins to become possible. It is suggested that the IR spectrum displayed in **Fig. 5**(b) and **Fig. 5**(c) are solidly indicated that proteins have denatured on all UHMWPE composite samples. However, since the difference is not too apparent, thus, no further conclusion related to the samples' wear properties can be simply deduced. Yet, it can be concluded that the conformations of proteins can happen at static conditions by providing favorable solid surface properties for the proteins to initially get adsorbed and sufficient time. From this point of view, it was suggested that the deterioration of the UHMWPE composite can be triggered by the physicochemical interactions between the proteins and the implant materials without the involvement of external stresses or the patient's activity (varies contact load).

Although this theory could be applicable for this particular static condition, the interaction of proteins on the modified UHMWPE composite under the practical conditions in the hip joint application is still debatable. The introduction of UHMWPE composites into the hip joint application could lead to a new mechanism of protein interactions with the UHMWPE composite surface. Henceforth, the multidirectional wear sliding test was performed. The proteins adsorption on the UHMWPE composite's surface were evaluated and analysed.

3.2 Multidirectional wear sliding test

3.2.1 Specific wear rate

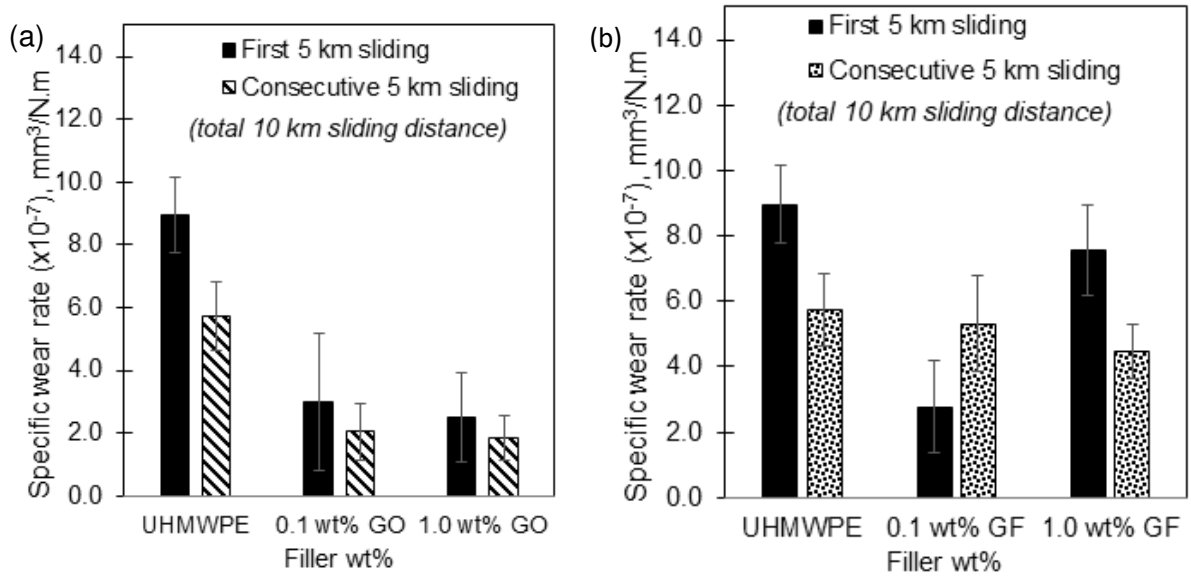

Fig. 6. Comparison of specific wear rate between the UHMWPE and (a) UHMWPE/GO, (b) UHMWPE/GF after 5 km and 10 km sliding distance under 5 MPa contact load,

Fig. 6 showed the calculated specific wear rate for each sample. The specific wear rate was calculated according to their sliding distance, which is the first 5 km and the final 5 km sliding distance. During the first 5 km sliding distance, **Fig. 6**(a) showed that the wear rate of UHMWPE was yield to be 8.95×10^{-7} mm^3/Nm. Followed by the UHMWPE/0.1GO and UHMWPE/1.0 GO that displayed a significant reduction of about 2.98×10^{-7} mm^3/Nm and 2.51×10^{-7} mm^3/Nm, respectively. The wear rate has remarkably reduced by 67% and 72%, respectively. Meanwhile, after completed the final 5 km sliding, the UHMWPE showed a slight reduction by 36%. The same reduction trend was also yielded by both UHMWPE/0.1GO and UHMWPE/1.0GO after completed the final 5 km sliding distance; 31% and 27%, respectively. This implied that the UHMWPE and UHMWPE/GO sample have undergone a steady-state of wear after sliding the final 5 km sliding distance.

On the other hand, in **Fig. 6**(b), after completing the first 5 km sliding, the specific wear rate of UHMWPE/0.1GF and UHMWPE/1.0GF yielded about 2.78×10^{-7} mm^3/Nm and 7.57×10^{-7} mm^3/Nm, respectively. The wear rate was compared to the UHMWPE and reduced by 69% and 15%, respectively. By completed the final 5 km sliding, the wear rate of UHMWPE/0.1GF has increased to 5.32×10^{-7} mm^3/Nm, which has dramatically increased by

92%. Meanwhile, UHMWPE/1.0GF has shown wear rate reduction of about 4.45×10^{-7} mm^3/Nm (41%). This suggested that the UHMWPE/1.0GF has undergone the steady-state of wear, whereas the UHMWPE/0.1GF probably has undergone accelerated wear. Since the sliding distance was only limited to 10 km, hence, no further conclusion can be achieved from the graph. Therefore, evaluation on the worn surfaces was done using both optical microscope and scanning electron microscope as complementary data. The sample was analysed concerning the influence of their filler types and the effect of the contact load during the wear sliding test.

3.2.2 Worn surface of modified UHMWPE

The following **Fig. 7** displayed the worn surfaces of each sample after performing wear test of the first 5 km and the last 5 km sliding distance. The micrographs were obtained at the aperture of 400 µm × 400 µm using an optical microscope. The first **Fig. 7**a(i) showed UHMWPE's worn surface that has removed some of its machining marks during the first 5 km sliding distance. After completed the last 5 km sliding, all machining marks are mostly removed and left the surface to become smoother. Some protuberance surface structures can also be observed in **Fig. 7**a(ii). This structure is usually related as an indication of an overheating phenomenon [19], leading to the toughening of the material. Moreover, the protuberance formation was usually observed when the peak load is higher than 2 MPa results temperature elevation at contact spots [19].

In **Fig. 7**b(i), UHMWPE/0.1GO showed the machining marks has become a blur and spotty. However, according to its wear loss value during the early sliding, only 0.093 mm^3 wear was a loss. This suggested that the machining mark was deformed instead of removed which explained the structure changes (blurred lines, and spots). Interestingly, after continuing the sliding distance, the UHMWPE/0.1GO in **Fig. 7**b(ii), showed a protuberance structure that arose from the ring pattern of the machining marks in the earlier sliding. The higher amount of protuberance structure observed on the surface has correspondingly reduced the wear rate of the UHMWPE/0.1GO by 64%. In addition, at the worn surface of UHMWPE/1.0GO in **Fig. 7**c(i), its surface appeared to have almost the same appearance with the UHMWPE in **Fig. 7a**(i), However, the machining marks in **Fig. 7**c(i), was appealed to be blurred compared to the defined machining lines on **Fig. 7**a(i). There was no protuberance structure can be detected on **Fig. 7**c(i), surface, and the machining marks remnant can be detected where the GO fillers spotted. This suggested that the existence of GO filler near the sliding surface has improved

the subsurface strength of the material, thus increased its wear resistivity. Furthermore, the GO filler which had high thermal conductivity has also influence improved the heat dissipation on the surface during sliding activities. The improved heat dissipation has reduced the heat elevation on the contact points of the surface, thus, inhibit the formation of the protuberance. Despite that, the wear removal is very low compared to the UHMWPE/0.1GO and the UHMWPE; 0.078 mm^3. Moreover, after completed the last 5 km sliding, the UHMWPE/1.0GO in **Fig. 7**c(ii), showed almost the same protuberance structure as in **Fig. 7**b(ii). The wear rate of UHMWPE/1.0GO has reduced by 11% compared to the UHMWPE/0.1GO suggested that the combined effect of protuberance structure and the reinforcement of higher GO percentage has extended the wear rate reduction.

On the other hand, at the early sliding of UHMWPE/0.1GF; **Fig. 7**d(i), protuberance structure and discolored spots can be observed on the worn surface. After performing the last 5 km sliding, UHMWPE/0.1GF; **Fig. 7**d(ii), the protuberance structure has arisen more evidently in more random patterns. Moreover, the increment of discolored spots can also be observed indicated higher subsurface cracking (inferior cracks). Although the discolored spots were detected at the early sliding, the wear rate was only increased after performed the last 5 km sliding. This suggested that the protuberance structure has played a great role in toughening the surface materials, thus promoted wear resistivity.

Meanwhile, the UHMWPE/1.0GF in **Fig. 7**e(i), displayed the formation of a protuberance structure on its surface after the first 5 km sliding. The protuberance structure was observed to form on the lighter surface region when the actual sample color is black. After the last 5 km sliding, the UHMWPE/1.0GF sample has shown almost the same surface appearance as its initial sliding. The most evident structure that arises on the UHMWPE/1.0GF was protuberance. The protuberance structure which was formed due to elevated thermal at the contact points have emerged and forming hardened surface points. The hardened surface points were responsible for reducing the wear loss during sliding activities. Although the UHMWPE/1.0GF has a protuberance structure since the early sliding distance, the wear loss was higher than the UHMWPE/0.1GF. However, by observing more critically, there was a light surface region underlying beneath protuberance within the material. This indicated that the high wear rate was caused by the subsurface cracking. The existence of protuberance was suggested to have inhibited the propagation of the subsurface cracks, thus, limits its wear volume production. The remnants of the protuberance were further used to resist the shear stress from the counterface material, which reflects on the wear reduction of UHMWPE/1.0GF

after the final 5 km sliding. The surface in **Fig. 7**e(ii), has also shown an apparent reduction of protuberance structure. Conclusively, the protuberance structure which exclusively emerged during the sliding test at 5 MPa contact load has conveniently toughened the surface composites. Leading to the reduction of the wear rate.

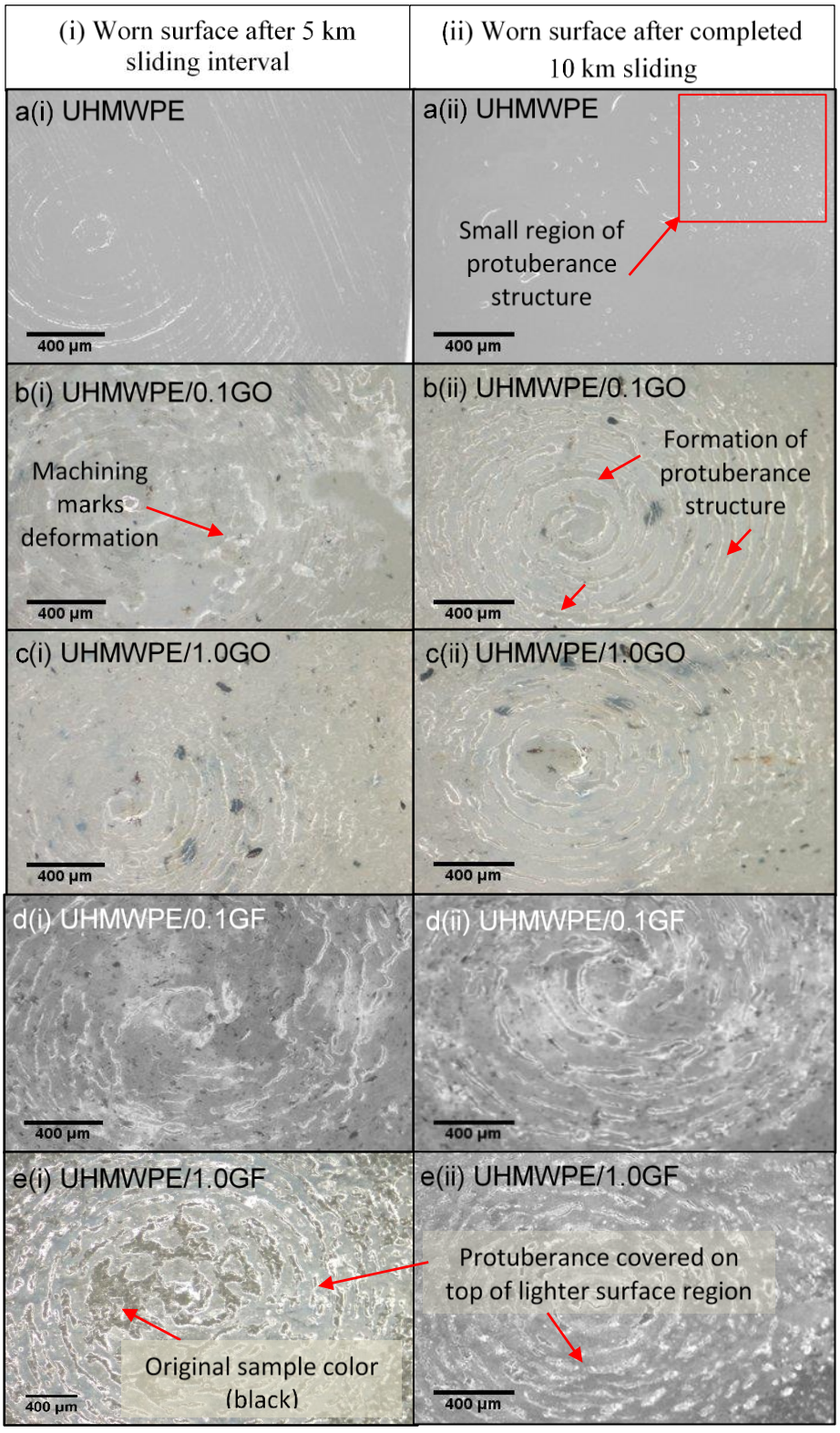

Fig.7. Comparison of optical micrographs from worn surface of UHMWPE and UHMWPE coposites pin sample (i) after the first 5 km sliding distance and (ii) after the finishing 10 km sliding distance under contact load 5 MPa.

3.2.3 Protein adsorption analysis post sliding

The protein's conformation was analyzed at the amide spectrum in the range of 1800-1500 cm^{-1} using the FTIR spectroscopy after the wear test as shown in **Fig. 8**.

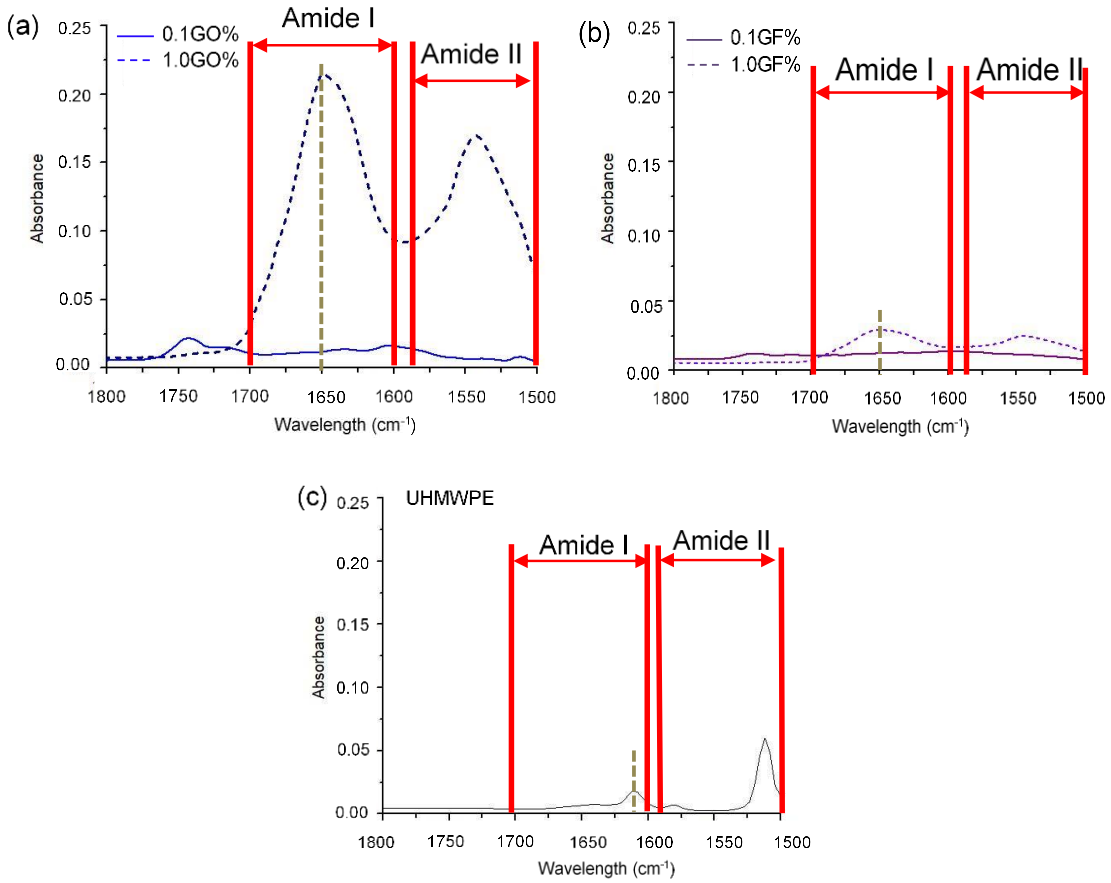

Fig. 8. ATR-FTIR spectra of proteins after 10 km sliding distance of 30 v/v bovine serum lubricated condition, (a) UHMWPE/0.1GO and UHMWPE/1.0GO, (b) UHMWPE/0.1GF and UHMWPE/1.0GF, (c) UHMWPE.

Referring to **Fig. 8**(a) and **Fig. 8**(b) it shows that the UHMWPE composite reinforced with low filler concentration; 0.1 wt% have shown a featureless IR spectrum within the peak range of amide I (1700-1600 cm^{-1}). Almost the same IR spectra feature of amide I can be observed in **Fig. 8**(c) which detected on the UHMWPE surface. It is also displayed a weak peak of amide I IR spectrum and the shifted peak was detected at amide I spectrum from originally centered at 1650 cm^{-1} to 1613 cm^{-1}. The 1613 cm^{-1} shifted peak is corresponding to the amino acid's side chain adsorption which indicated as some fraction of the proteins sustaining their secondary structure although major fraction has severely denatured [44].

The featureless amide I spectra is usually obtained from the unfolded protein structure. The denatured proteins have lost their original secondary structures under the sliding condition which closely linked from the thermal denaturation or frictional shearing [45]. Proteins denaturation can be caused by the rising temperature at the exact sliding real contact area where the friction is at the highest. The proteins adsorbed in the area surrounding is affected by the heat generated and becomes denatured [5,43,45]. In contrast, the UHMWPE composites reinforced with higher filler percentage (1.0 wt%) have shown a distinct peak as shown in **Fig.8**(a), but relatively weak peak in **Fig.8**(b), which suggested that very less denatured proteins were detected on their surface, especially on the UHMWPE/1.0GO surface. Meanwhile, the UHMWPE/1.0GF has shown a dwindled peak at least 9 times less than the UHMWPE/1.0GO's peak of amide I spectra. The influence of high thermal properties of both GO and GF may be attributed to heat dissipation on the surface during the sliding conditions [11,18], and it required a sufficient amount of GO and GF for the heat dissipating effect to take place. However, even at the same filler percentage as GO, the UHMWPE/1.0GF's surface was still displaying higher denatured proteins as portrayed from the lower peak intensity of secondary structure compared to UHMWPE/1.0GO. It was suspected that the difference in thermal conductivity of each sample played a different role in protein denaturation on each surface. Therefore, the thermal conductivity of each sample was investigated using DSC.

3.3 Thermal conductivity analysis

Thermal conductivity is quantified by the thermal conduction parameter in W/m.K, defining how fast a material can diffuse heat. From a mathematical perspective, a fraction of thermal energy, Q would diffuse into the material within a certain amount of time, t. By getting through the thickness of the material and perpendicularly diffuse to the opposite surface area, the ease of heat to get conducted through the material was measured using the **Equation (4)**.

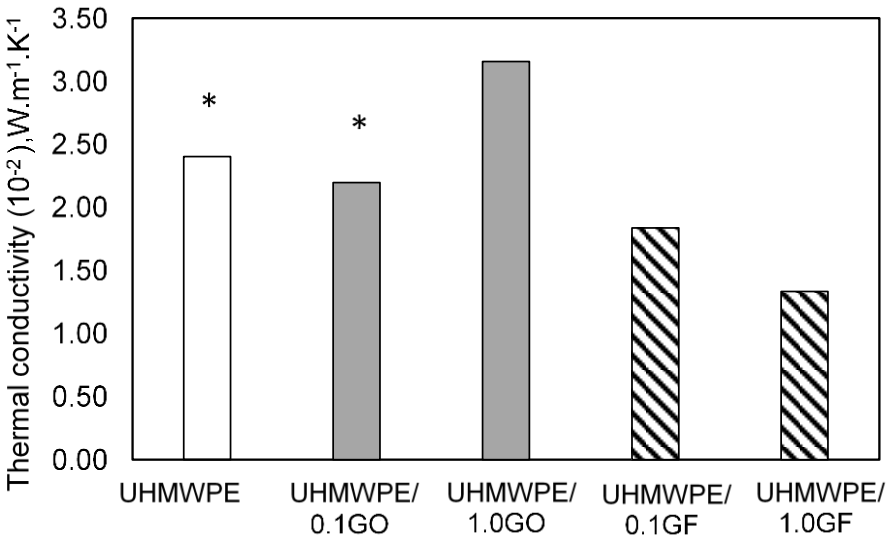

Fig.9. Thermal conductivity of UHMWPE, UHMWPE/GO and UHMWPE/GF composites at different filler contents; where (*) denotes no significant difference ($p>0.05$).

Fig. 9 showed the magnitude of the thermal conductivity of UHMWPE based composites filled with GO and GF at increasing filler content. The incorporation of GO has displayed a significant thermal conductivity increment at 1.0 wt%. The incorporation of GO at 0.1 wt% displayed a slight reduction by 8% (2.198×10^{-2} W/m.K) compared to the UHMWPE. The thermal conductivity reduction can be perceived to have the same thermal conductivity as the UHMWPE, due to the insignificant difference value, $p> 0.05$. Moreover, the reinforcement of 1.0 wt% GO has effectively increased the thermal conductivity of the UHMWPE (2.403×10^{-2} W/m.K) by 32%. The increment of the thermal conductivity was suggested due to the effective formation of a thermal path for the heat to diffuse across the highly thermal conductive GO filler (5000 W/m.K). The shorter duration for heat diffusion led to higher heat dissipation which reducing the protein denaturation as a result of elevated heat during the articulating activities. The effective heat dissipation was then translated via the previous FTIR spectrum in **Fig. 8** which shows the lowest magnitude of proteins has denatured on the UHMWPE/1.0GO surface.

On the other hand, reinforcement of GF into UHMWPE displayed an unexpected reduction of thermal conductivity. The measurement revealed that when 0.1 wt% GF was loaded into the UHMWPE, thermal conductivity was reduced by 25% (1.84×10^{-2} W/m.K) compared to the UHMWPE. The thermal conductivity was observed to be further reduced by 45% when 1.0 wt% GF was loaded (1.33×10^{-2} W/m.K). This finding was unexpected as GF

has a thermal conductivity of about 3000 W/m.K [46]. In addition to that, referring to previous studies [11,13,47], the reinforcement of high thermal conductivity fillers such as carbon nanotube (CNT) and graphene nanoplatelet (GNP) has effectively increased the thermal conductivity of the polymer composites with minimum requirement of 14 wt% filler volume. Although the amount of filler used in this study was not enough to achieve a great thermal conductivity increment [11,18,47], it was expected to achieve the same magnitude of thermal conductivity as the UHMWPE at the very least. Therefore, the evident reduction of thermal conductivity when GF was reinforced, suggested being influenced by other factors such as crystal defects and the reduction of crystallinity percentage. Hence, during the thermal diffusion, the heat would be largely scattered due to randomly mannered chains, thus reducing the heat dissipation of the articulating surface [11]. This has largely reduced the thermal conductivity values of UHMWPE/GF. The low thermal conductivity affected low heat dissipation, thus allowing proteins to become denatured from the elevated thermal produced by the articulating surface activities.

4.0 Conclusions

This work is focused on investigating the influence of protein interaction towards the UHMWPE filled with graphitic materials (GO and GF) at varying concentrations (0.1 wt%, 1.0 wt%). The conclusions were drawn as followed:

1) The reinforcement of the graphitic fillers; UHMWPE/GO and UHMWPE/GF has shown a slight reduction of hydrophobicity proven from the deflation of the contact angle on their surface compared to the UHMWPE by 6.7% and 10.5%, respectively. The interaction on the UHMWPE composite's surface was dominated by physical interaction instead of the physicochemical interaction. Thereupon, vary filler concentrations has no significant effect on further improving the UHMWPE composite's wettability.

2) The reinforcement of the GF in the UHMWPE has altered its surface charge to become mutual with the BSA protein's charge. Whereas, UHMWPE/GO's surface charge remained the same as the UHMWPE. The UHMWPE/GF was proven to have successfully minimized the protein interaction in a static condition with increasing GF content; 1.47% and 0.07%, respectively.

3) Interestingly, although there was only small fractions of protein get interacted on the UHMWPE/GF surface, the denatured proteins on its surface is considerably higher compared to the UHMWPE/GO surface referring to their FTIR amide peaks due to its lower thermal conductivity suggesting slower rate of heat dissipation during the articulating activities.

4) GO has a significantly reduced wear rate by 58.88% compared to GF when using at the same concentration (1.0 wt%) in UHMWPE. The combined effect of protuberance structure and the existence of GO filler near the sliding surface has improved the subsurface strength of the material, thus increased its wear resistivity. Furthermore, the GO filler which had high thermal conductivity reducing the protein denaturation as a result of elevated heat during the articulating activities.

Acknowledgments

The authors express a high gratification to the sponsor; Malaysia-Japan International Institute for funding trip to Kyushu University and have made the collaboration project possible. This research is supported by the grant from the Ministry of Higher Education Malaysia [Grant number: R.K130000.7843.5F085].

References

1. Ingham, E., Fisher, J.: The role of macrophages in osteolysis of total joint replacement. Biomaterials 26(11) (2005). https://doi.org/10.1016/j.biomaterials.2004.04.035
2. Baena, J.C., Wu, J., Peng, Z.: Wear performance of UHMWPE and reinforced UHMWPE composites in arthroplasty applications: A review. Lubricants 3(2) (2015). https://doi.org/10.3390/lubricants3020413
3. Chukov, D.I., Stepashkin, A.A., Maksimkin, A.V., Tcherdyntsev, V.V., Kaloshkin, S.D., Kuskov, K.V., Bugakov, V.I.: Investigation of structure, mechanical and tribological properties of short carbon fiber reinforced UHMWPE-matrix composites. Compos. B. Eng. 76 (2015). https://doi.org/10.1016/j.compositesb.2015.02.019
4. Salari, M., Taromsari, S.M., Bagheri, R., Sani, M.A.F.: Improved wear, mechanical, and biological behavior of UHMWPE-HAp-zirconia hybrid nanocomposites with a prospective application in total hip joint replacement. J. Mater. Sci. 54(5) (2019). https://doi.org/10.1007/s10853-018-3146-y
5. Karuppiah, K.S.K., Sundararajan, S., Xu, Z.H., Li, X.: The effect of protein adsorption on the friction behavior of ultra-high molecular weight polyethylene. Tribol. Lett. 22(2) (2006). https://doi.org/10.1007/s11249-006-9078-8

6. Sawae, Y., Yamamoto, A., Murakami, T.: Influence of protein and lipid concentration of the test lubricant on the wear of ultra high molecular weight polyethylene. Tribol. Int. 41(7) (2008). https://doi.org/10.1016/j.triboint.2007.11.010
7. Ghosh, S., Choudhury, D., Das, N.S., Pingguan-Murphy, B.: Tribological role of synovial fluid compositions on artificial joints - a systematic review of the last 10 years. Lubr. Sci. 26(6) (2014). https://doi.org/10.1002/ls.1266
8. Gu, J., Li, N., Tian, L., Lv, Z., Zhang, Q.: High thermal conductivity graphite nanoplatelet/UHMWPE nanocomposites. RSC Adv. 5(46) (2015). https://doi.org/10.1039/c5ra03284a
9. Tahir, N.A.M., Abdollah, M.F.B., Tamaldin, N., Amiruddin, H., Zin, M.R.B.M.:. A brief review on the wear mechanisms and interfaces of carbon based materials. Compos. Interfaces 25(5-7) (2018). https://doi.org/10.1080/09276440.2018.1380472
10. Vadivel, H.S., Golchin, A., Emami, N.: Tribological behaviour of carbon filled hybrid UHMWPE composites in water. Tribol. Int. 124 (2018). https://doi.org/10.1016/j.triboint.2018.04.001
11. Burger, N., Laachachi, A., Ferriol, M., Lutz, M., Toniazzo, V., Ruch, D.: Review of thermal conductivity in composites: Mechanisms, parameters and theory. Prog. Polym. Sci. 61 (2016). https://doi.org/10.1016/j.progpolymsci.2016.05.001
12. Suñer, S,, Emami, N.: Investigation of graphene oxide as reinforcement for orthopaedic applications. Tribol. Mater. Surf. Interfaces 8(1) (2014). https://doi.org/10.1179/1751584X13Y.0000000053
13. Kumar, R.M., Sharma, S.K., Kumar, B.V.M., Lahiri, D.:. Effects of carbon nanotube aspect ratio on strengthening and tribological behavior of ultra high molecular weight polyethylene composite. Compos. Part. A-Appl. S. 76 (2015). https://doi.org/10.1016/j.compositesa.2015.05.007.
14. Ashraf, M.A., Peng, W., Zare, Y., Rhee, K.Y.: Effects of size and aggregation/agglomeration of nanoparticles on the interfacial/interphase properties and tensile strength of polymer nanocomposites. Nanoscale Res. Lett. 13 (2018). https://doi.org/10.1186/s11671-018-2624-0
15. Pang, W., Ni, Z., Wu, J.L., Zhao, Y.: Investigation of tribological properties of graphene oxide reinforced ultrahigh molecular weight polyethylene under artificial seawater lubricating condition. Appl. Surf. Sci. 434 (2018). https://doi.org/10.1016/j.apsusc.2017.10.115
16. Kitazaki, Y., Hata, T.: Surface-chemical criteria for optimum adhesion. J. Adhes. 4 (1972). https://doi.org/10.1080/00218467208072217
17. Hata, T., Kitazaki, Y., Saito, T.: Estimation of the surface energy of polymer solids. J. Adhes. 21 (1987). https://doi.org/10.1080/00218468708074968
18. Shrivastava, A.: Introduction to plastics engineering. Plastics Design Library (2018). https://doi.org/10.1016/b978-0-323-39500-7.00001-0
19. Saikko, V.: Effect of contact pressure on wear and friction of ultra-high molecular weight polyethylene in multidirectional sliding. Proc. Inst. Mech. Eng. Pt. H. J. Eng. Med. 220(7) (2006) https://doi.org/10.1243/09544119JEIM146

20. Chalernpon, K., Aroonjarattham, P., Aroonjarattham K.: Static and dynamic load on hip contact of hip prosthesis and thai femoral bones. Int. J. Mech. Mechatron. Eng. 9(3) (2015). https://doi.org/10.5281/zenodo.1099670
21. Kitano, T., Ohashi, H., Kadoya, Y., Kobayashi, A., Yutani, Y., Yamano, Y.: Measurements of ζ potentials of particulate biomaterials in protein - rich hyaluronan solution with changes in pH and protein constituents. J. Biomed. Mater. Res. A. 42(3) (1998). https://doi.org/10.1002/(SICI)1097-4636(19981205)42:3<453::AID-JBM15>3.0.CO;2-H
22. Nakanishi, K., Sakiyama, T., Imamura, K.: On the adsorption of proteins on solid surfaces, a common but very complicated phenomenon. J. Biosci. Bioeng. 91(3) (2001). https://doi.org/10.1016/S1389-1723(01)80127-4
23. Choudhury, D., Ranuša, M., Fleming, R.A., Vrbka, M., Křupka, I, Teeter, M.G., Goss, J., Zou, M.: Mechanical wear and oxidative degradation analysis of retrieved ultra-high molecular weight polyethylene acetabular cups. J. Mech. Behav. Biomed. Mater. 79 (2018). https://doi.org/10.1016/j.jmbbm.2018.01.003
24. Shahemi, N., Liza, S., Abbas, A.A., Merican, A.M.: Long-term wear failure analysis of UHMWPE acetabular cup in total hip replacement. J. Mech. Behav. Biomed. Mater. 87 (2018). https://doi.org/10.1016/j.jmbbm.2018.07.017
25. Parkes, M., Myant, C., Cann, P.M., Wong, J.S.S.: Synovial fluid lubrication: the effect of protein interactions on adsorbed and lubricating films. Biotribology. 1-2 (2015) https://doi.org/10.1016/j.biotri.2015.05.001
26. Murakami, T., Yarimitsu, S., Sakai, N., Nakashima, K., Yamaguchi, T., Sawae, Y.: Importance of adaptive multimode lubrication mechanism in natural synovial joints. Tribol. Int. 113 (2017) https://doi.org/10.1016/j.triboint.2016.12.052
27. Rabe, M., Verdes, D., Seeger, S.: Understanding protein adsorption phenomena at solid surfaces. Adv. Colloid. Interface. Sci. 162(1-2) (2011). https://doi.org/10.1016/j.cis.2010.12.007
28. Pandey, P.R., Roy, S., Is it possible to change wettability of hydrophilic surface by changing its roughness? J. Phys. Chem. Lett. 4(21) (2013). https://doi.org/10.1021/jz401946v
29. Kumar, J.V., Rao, R.R.: Effects of surface roughness in squeeze film lubrication of spherical bearings. Procedia Eng. 127 (2015) 955-962. https://doi.org/10.1016/j.proeng.2015.11.442
30. Liza, S., Haseeb, A.S.M.A., Masjuki, H.H., Abbas, A.A., 2013. The wear behavior of cross- linked UHMWPE under dry and bovine calf serum-lubricated conditions. Tribol. Trans. 56(1), 130-140. https://doi.org/10.1080/10402004.2012.732199.
31. Myshkin, N., Kovalev, A., 2018. Adhesion and surface forces in polymer tribology-A review. Friction. 6(2), 143-155. https://doi.org/10.1007/s40544-018-0203-0.
32. Nečas, D., Sawae, Y., Fujisawa, T., Nakashima, K., Morita, T., Yamaguchi, T., Vrbka, M., Křupka, I., Hartl, M.: The influence of proteins and speed on friction and adsorption of metal/UHMWPE contact pair. Biotribology. 11 (2017). https://doi.org/10.1016/j.biotri.2017.03.003
33. Rahmati, M., Mozafari, M.: Protein adsorption on polymers. Mater. Today Commun. 17 (2018). https://doi.org/10.1016/j.mtcomm.2018.10.024

34. Mathé, C., Devineau, S., Aude, J.C., Lagniel, G., Chédin, S., Legros, V., Mathon, M.H., Renault, J.P. et al.: Structural determinants for protein adsorption/non-adsorption to silica surface. PLoS ONE. 8(11) (2013). https://doi.org/10.1371/journal.pone.0081346
35. Furuike, T., Chaochai, T., Komoto, D., Tamura, H.: Adsorption and desorption behaviors of bovine serum albumin on gelatin/chitosan sponge. J. Mater. Sci. Chem. Eng. 5(1) (2017).https://doi.org/10.4236/msce.2017.51015
36. Liao, C., Li, Y., Tjong, S.C.: Graphene nanomaterials: synthesis, biocompatibility, and cytotoxicity. Int. J. Mol. Sci. 19(11) (2018). https://doi.org/10.3390/ijms19113564
37. Sánchez-Sánchez, X., Elias-Zuñiga, A., Hernández-Avila, M., Processing of ultra-high molecular weight polyethylene/graphite composites by ultrasonic injection moulding: Taguchi optimization. Ultrason. Sonochem. 44 (2018). https://doi.org/10.1016/j.ultsonch.2018.02.042
38. Neogi, P., Wang, J.C.: Stability of two-destimensional growth of a packed body of proteins on a solid surface. Langmuir. 27(9) (2011). https://doi.org/10.1021/la104616b
39. Garcia-Seisdedos, H., Villegas, J.A., Levy, E.D.: Infinite assembly of folded proteins in evolution, disease, and engineering. Angew. Chem. Int. Ed. 58(17) (2019). https://doi.org/10.1002/anie.201806092
40. Wang, Y., Yin, Z., Li, H., Gao, G., Zhang, X.: Friction and wear characteristics of ultrahigh molecular weight polyethylene (UHMWPE) composites containing glass fibers and carbon fibers under dry and water-lubricated conditions. Wear. 380-381 (2017) https://doi.org/10.1016/j.wear.2017.03.006
41. Di Puccio, F., Mattei, L.: Biotribology of artificial hip joints. World. J. Orthop. 6(1) (2015). https://doi.org/10.5312/wjo.v6.i1.77
42. Nečas, D., Vrbka, M., Gallo, J., Křupka, I., Hartl, M.: On the observation of lubrication mechanisms within hip joint replacements. Part II: Hard-on-hard bearing pairs. J. Mech. Behav. Biomed. Mater. 89 (2019). https://doi.org/10.1016/j.jmbbm.2018.09.026
43. Roba, M., Naka, M., Gautier, E., Spencer, N.D., Crockett, R.: The adsorption and lubrication behavior of synovial fluid proteins and glycoproteins on the bearing-surface materials of hip replacements. Biomaterials. 30(11) (2009). https://doi.org/10.1016/j.biomaterials.2008.12.062
44. Baldassarre, M., Li, C., Eremina, N., Goormaghtigh, E., Barth, A.: Simultaneous fitting of absorption spectra and their second derivatives for an improved analysis of protein infrared spectra. Molecules 20(7) (2015). https://doi.org/10.3390/molecules200712599
45. Mishina, H., Kojima, M.: Changes in human serum albumin on arthroplasty frictional surfaces. Wear. 265(5-6) (2008). https://doi.org/10.1016/j.wear.2007.12.006
46. Anwar, Z., Kausar, A., Muhammad, B.: Polymer and graphite-derived nanofiller composite: An overview of functional applications. Polym. Plast. Technol. Eng. 55(16) (2016). https://doi.org/10.1080/03602559.2016.1163598
47. Han, Z., Fina, A.: Thermal conductivity of carbon nanotubes and their polymer nanocomposites: A review. Prog. Polym. Sci. 36(7) (2011). https://doi.org/10.1016/j.progpolymsci.2010.11.004

Figures

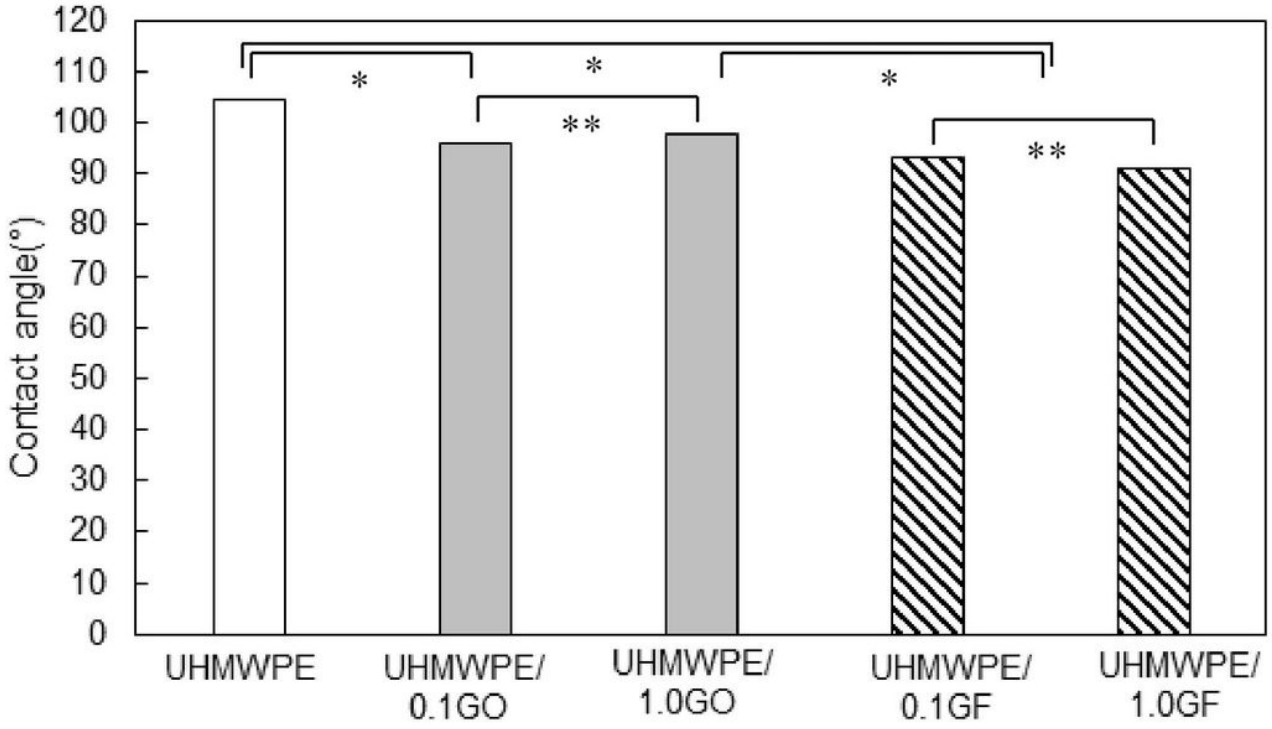

Figure 1

The contact angle of UHMWPE, UHMWPE/GO and UHMWPE/GF composites at different filler contents; where (*) denotes no significant difference ($p>0.05$) and (**) denotes significant difference ($p<0.05$)

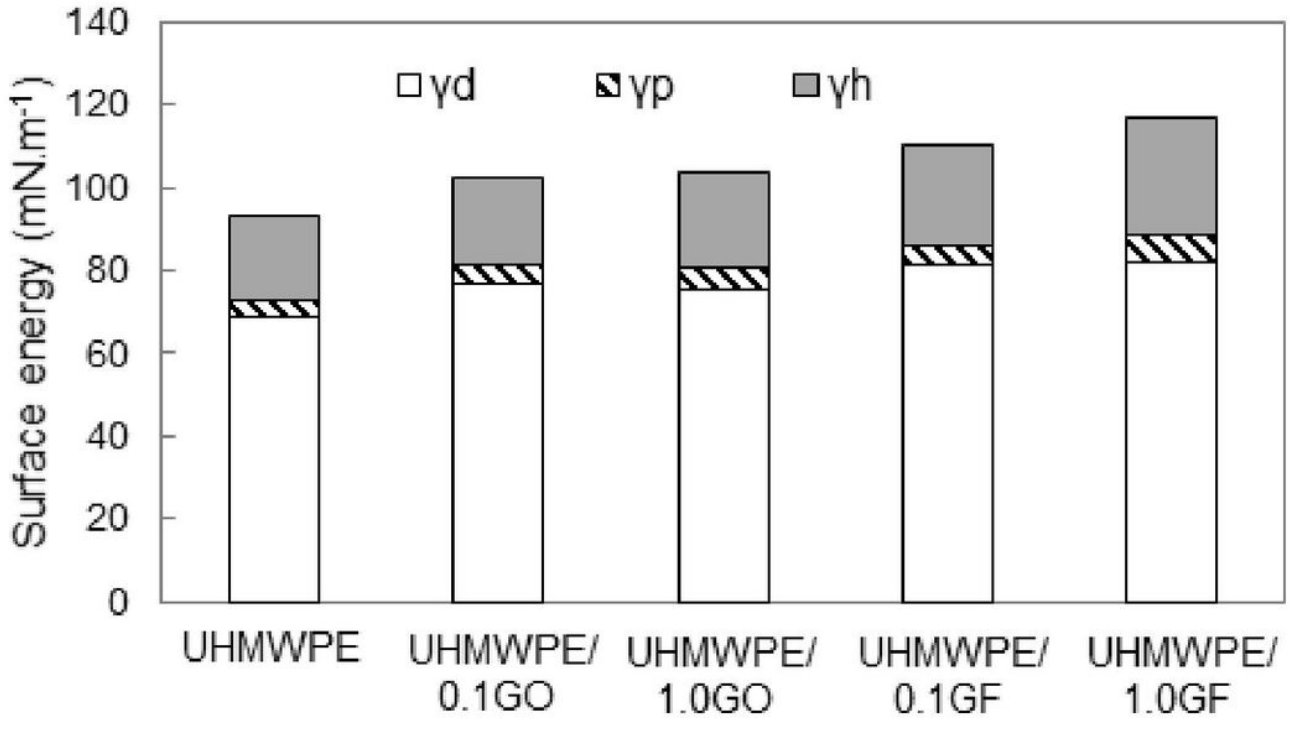

Figure 2

Surface free energy of UHMWPE and UHMWPE/GO and UHMWPE/GF composites at a different filler content

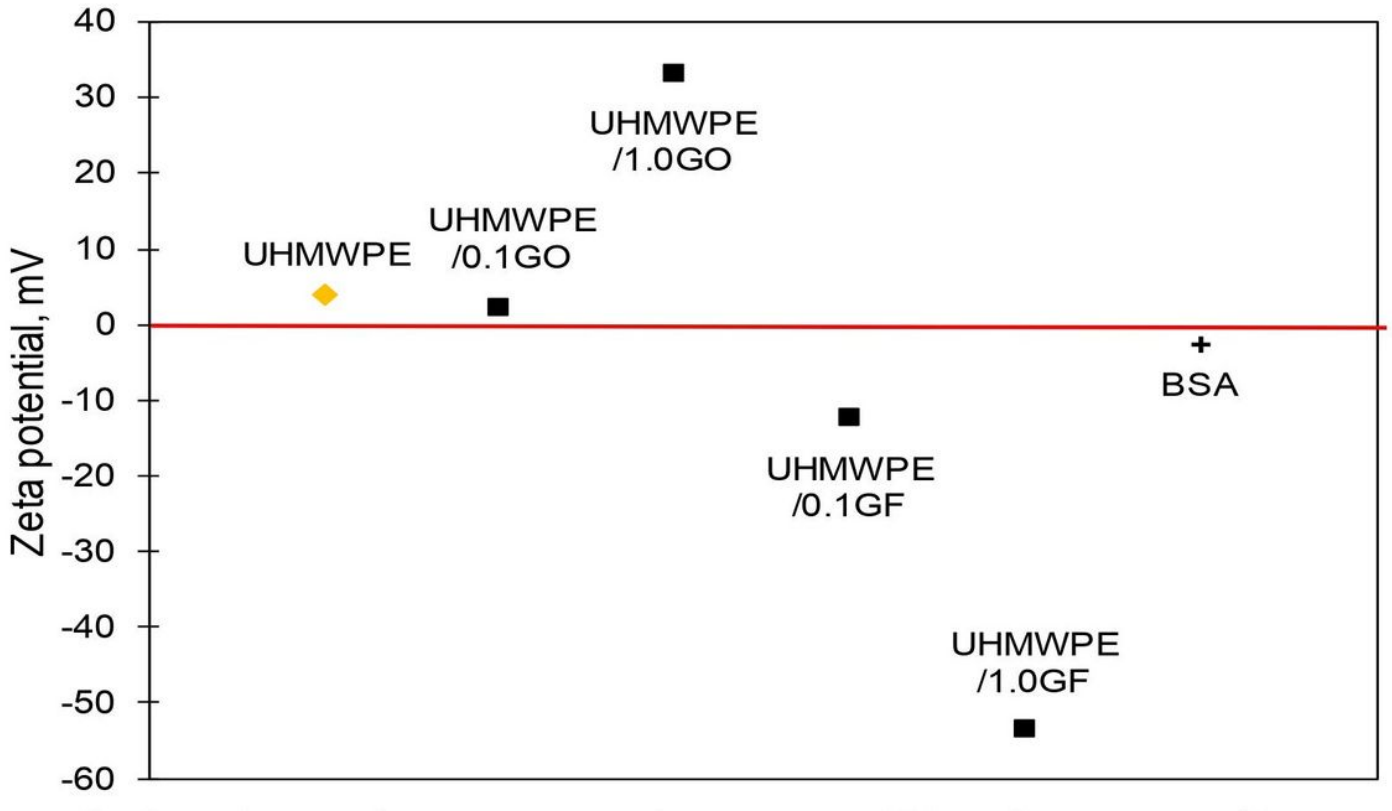

Figure 3

Surface charge of UHMWPE and UHMWPE/GO and UHMWPE/GF composites at different filler content.

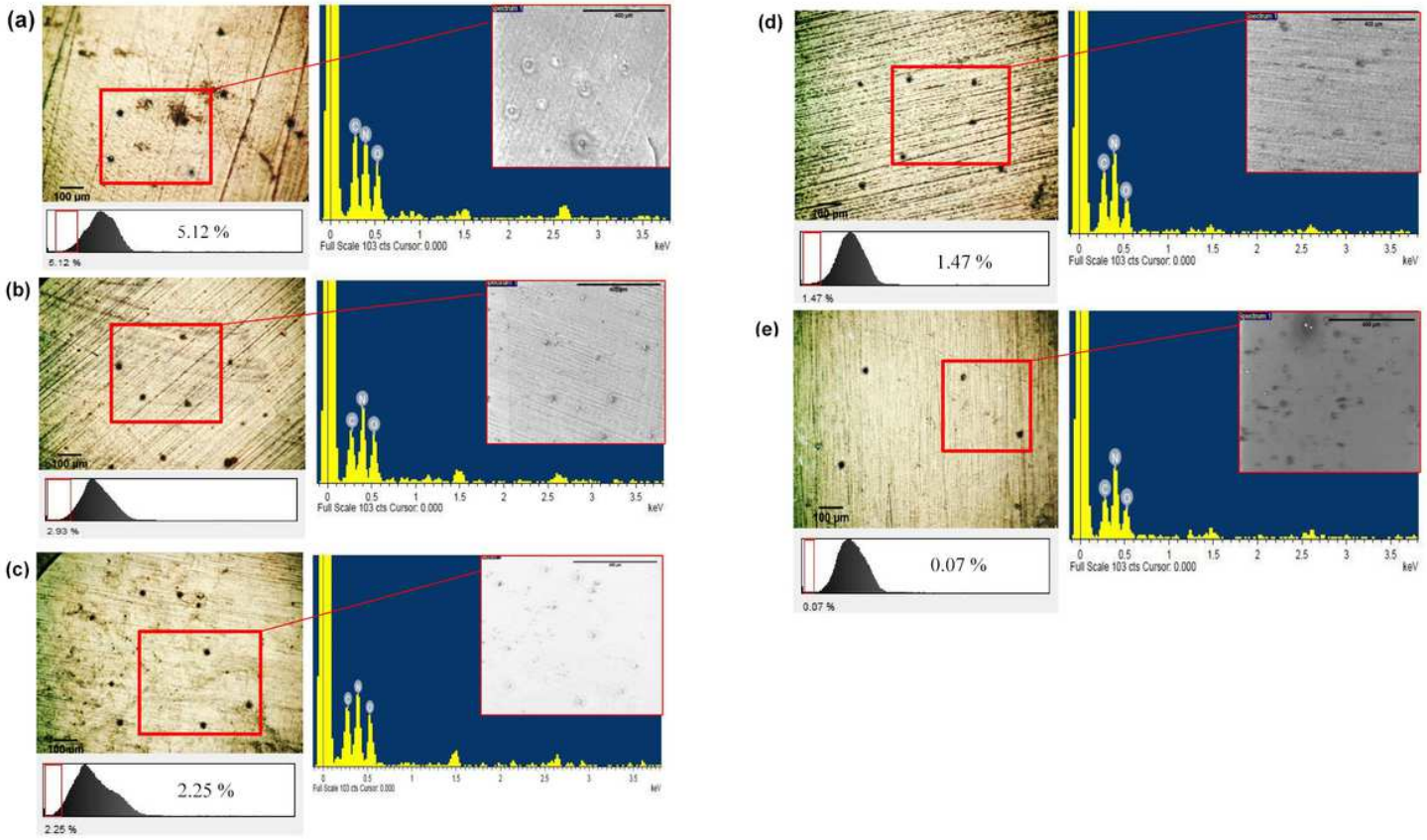

Figure 4

Optical micrographs showed protein coverage on each sample surface (a) UHMWPE, (b) UHMWPE/0.1GO, (c) UHMWPE/1.0GO, (d) UHMWPE/0.1GF, (e) UHMWPE/1.0GF after 24 hr of incubation.

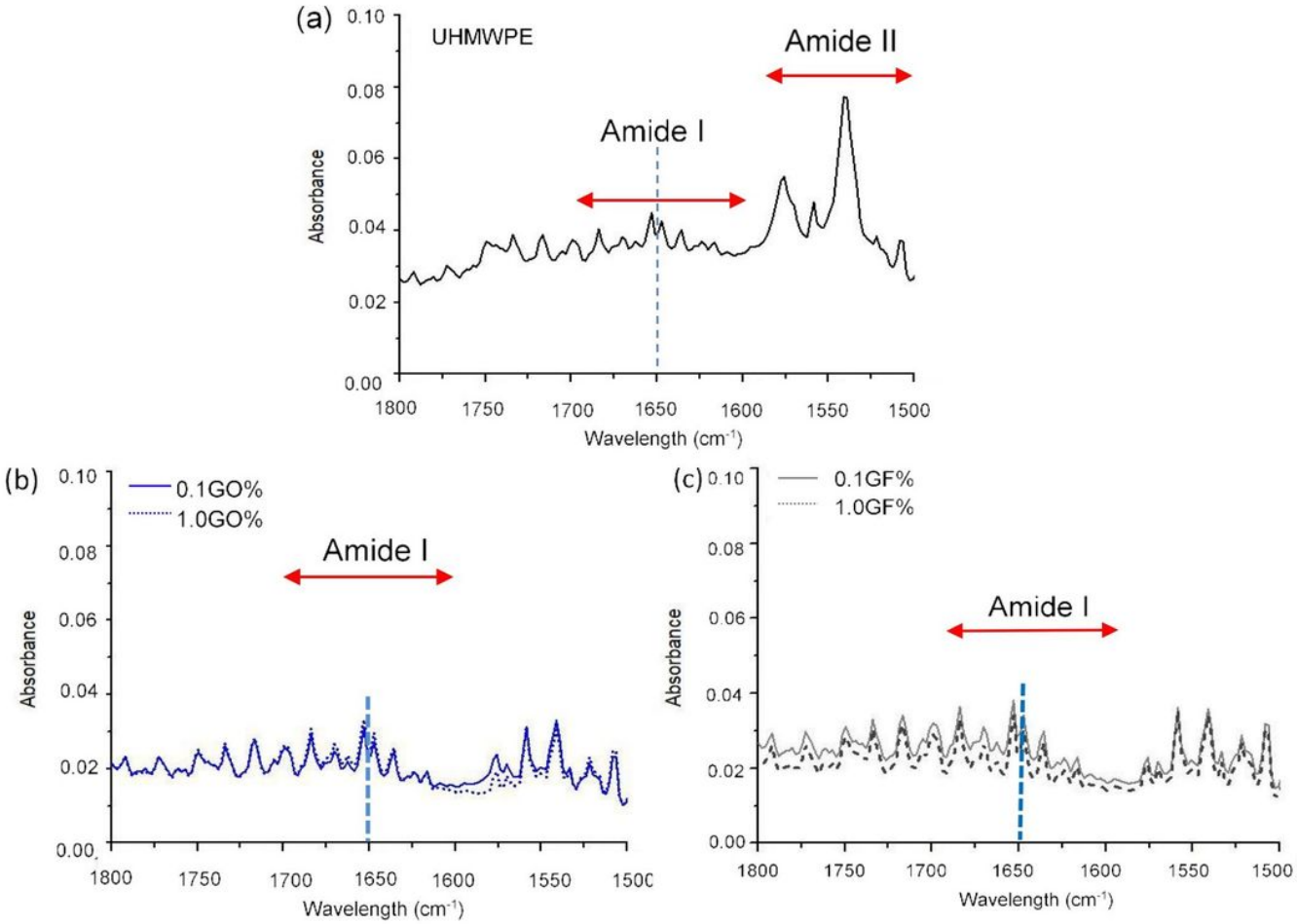

Figure 5

ATR-FTIR spectra of proteins after 24 hr static condition in 2 wt% of BSA solution, (a) UHMWPE, (b) UHMWPE/0.1GO and UHMWPE/1.0GO, (c) UHMWPE/0.1GF and UHMWPE/1.0GF.

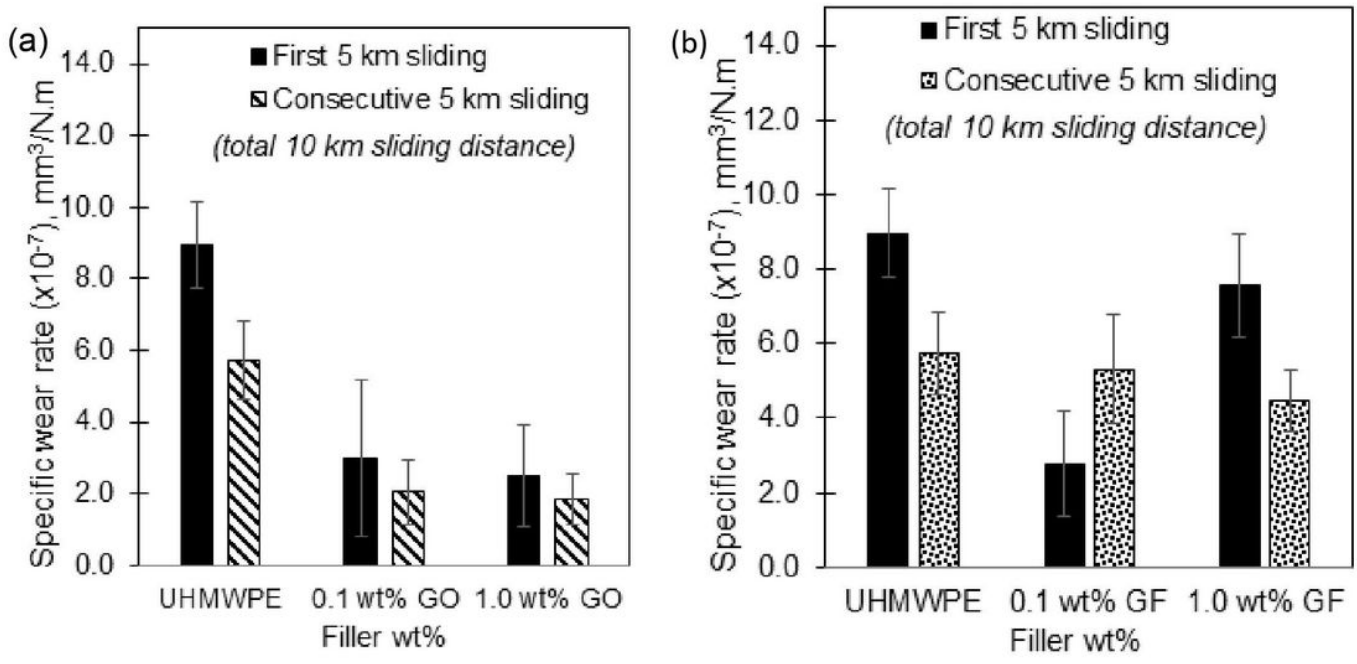

Figure 6

Comparison of specific wear rate between the UHMWPE and (a) UHMWPE/GO, (b) UHMWPE/GF after 5 km and 10 km sliding distance under 5 MPa contact load,

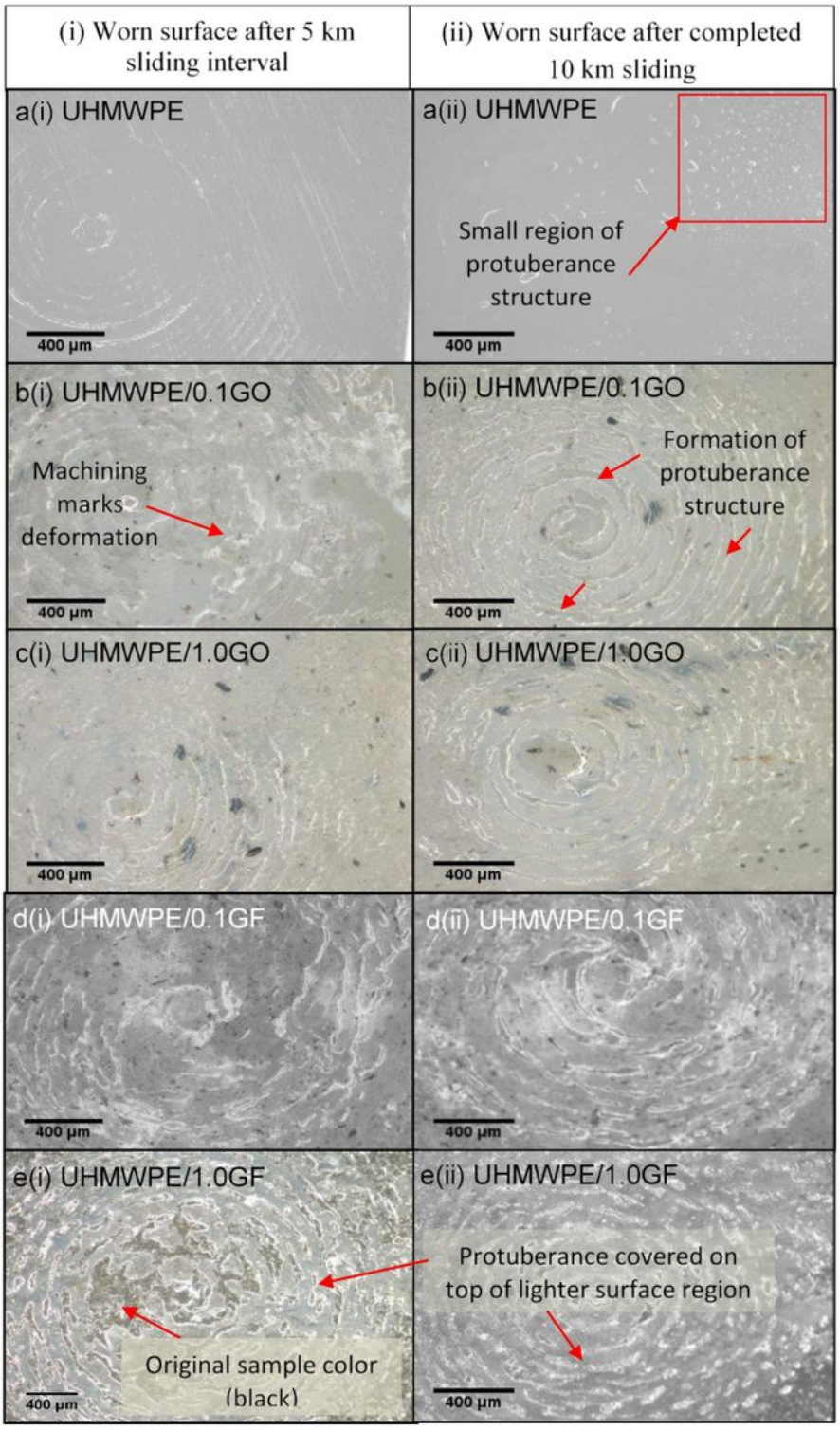

Figure 7

Comparison of optical micrographs from worn surface of UHMWPE and UHMWPE coposites pin sample (i) after the first 5 km sliding distance and (ii) after the finishing 10 km sliding distance under contact load 5 MPa.

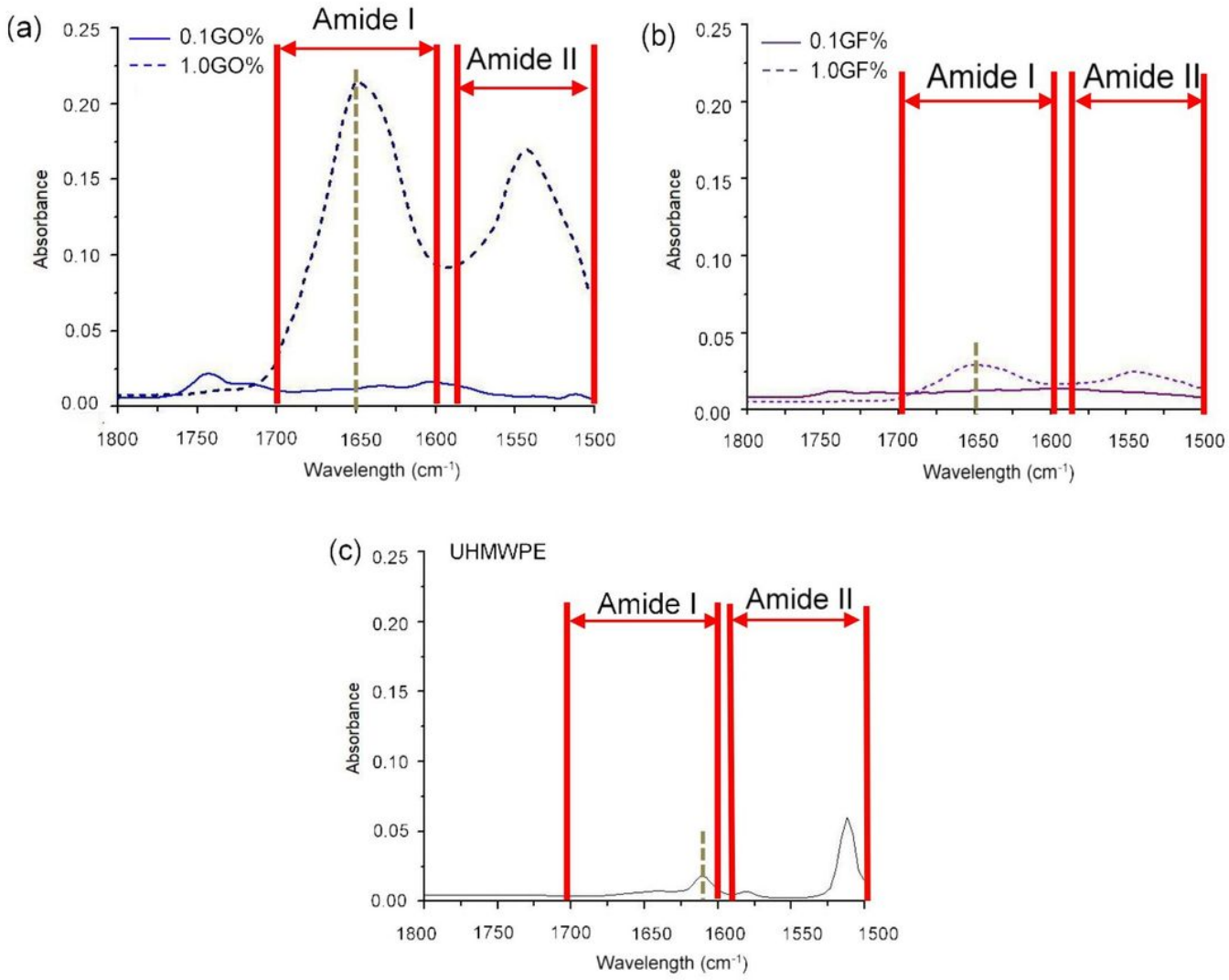

Figure 8

ATR-FTIR spectra of proteins after 10 km sliding distance of 30 v/v bovine serum lubricated condition, (a) UHMWPE/0.1GO and UHMWPE/1.0GO, (b) UHMWPE/0.1GF and UHMWPE/1.0GF, (c) UHMWPE.

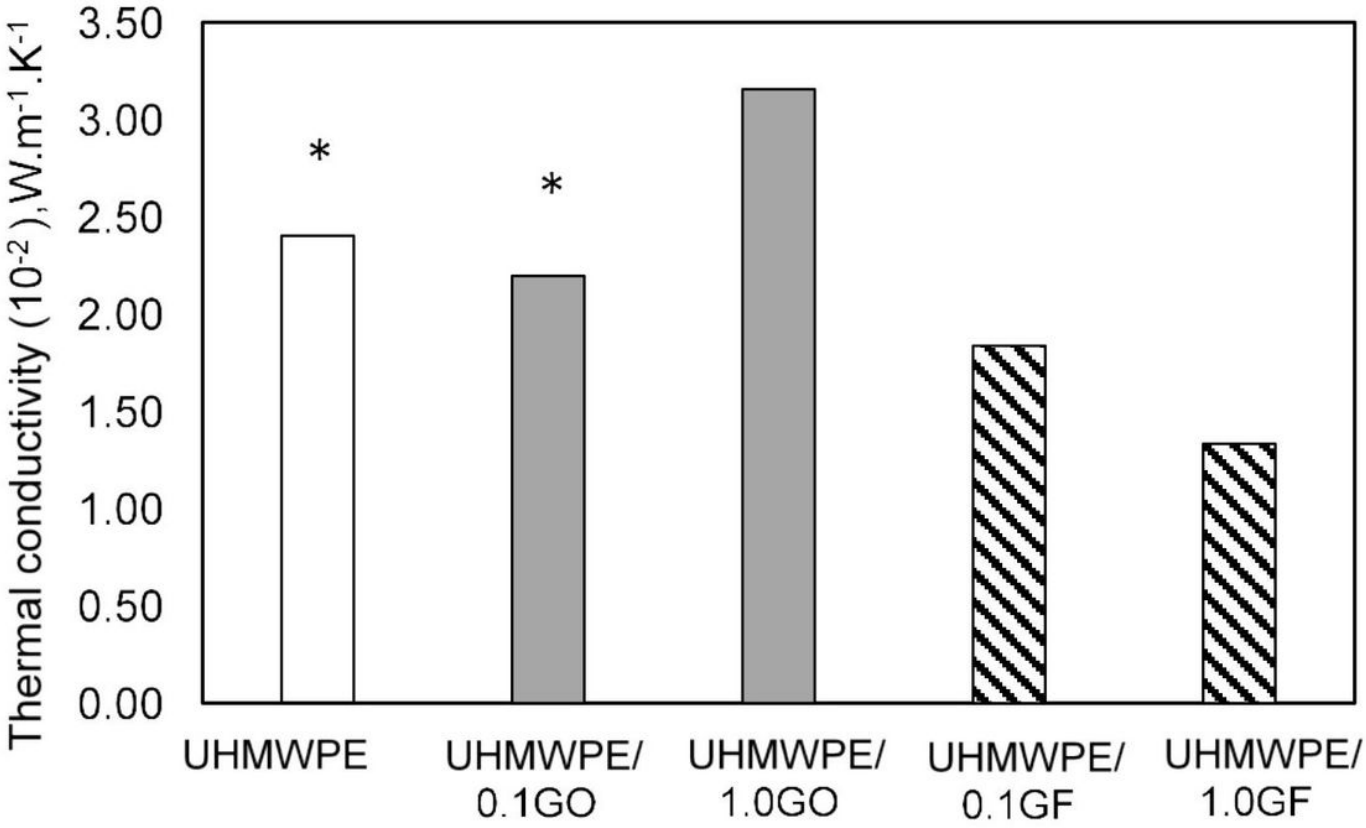

Figure 9

Thermal conductivity of UHMWPE, UHMWPE/GO and UHMWPE/GF composites at different filler contents; where (*) denotes no significant difference ($p>0.05$).